

Accelerated Structure Formation: the Early Emergence of Massive Galaxies and Clusters of Galaxies

STACY S. MCGAUGH,¹ JAMES M. SCHOMBERT,² FEDERICO LELLI,³ AND JAY FRANCK⁴

¹*Department of Astronomy, Case Western Reserve University, Cleveland, OH 44106, USA*

²*Institute for Fundamental Science, University of Oregon, Eugene, OR 97403, USA*

³*INAF – Arcetri Astrophysical Observatory, Largo Enrico Fermi 5, I-50125, Firenze, Italy*

⁴*1108 Sherman St., Longmont, CO 80501, USA*

ABSTRACT

Galaxies in the early universe appear to have grown too big too fast, assembling into massive, monolithic objects more rapidly than anticipated in the hierarchical Λ CDM structure formation paradigm. The available data are consistent with there being a population of massive galaxies that form early ($z \gtrsim 10$) and follow an approximately exponential star formation history with a short ($\lesssim 1$ Gyr) e-folding timescale on the way to becoming massive ($M_* \approx 10^{11} M_\odot$) galaxies by $z = 0$, consistent with the traditional picture for the evolution of giant elliptical galaxies. Observations of the kinematics of spiral galaxies as a function of redshift similarly show that massive disks and their scaling relations were in place at early times, indicating a genuine effect in mass that cannot be explained as a quirk of luminosity evolution. That massive galaxies could form by $z = 10$ was explicitly predicted in advance by MOND. We discuss some further predictions of MOND, such as the early emergence of clusters of galaxies and the cosmic web.

Keywords: Cold dark matter (265), Galaxy evolution (594), Galaxy formation (595), Galaxy masses (607), High-redshift galaxies (734), MOND (1069), Protogalaxies (1298)

1. INTRODUCTION

The formation and evolution of galaxies has been a central concern of cosmology since [Hubble \(1929\)](#) demonstrated that spiral nebulae are external stellar systems of size comparable to the Milky Way. Ideas about the formation of galaxies have ranged from the monolithic collapse of giant gas clouds ([Eggen et al. 1962](#)) to assembly through the merger of numerous protogalactic fragments ([Searle & Zinn 1978](#)). With the launch of JWST, we now have the opportunity to directly observing the assembly of galaxies at early epochs, providing a direct test of these ideas.

In Λ CDM, galaxies form in dark matter halos that originate from primordial density fluctuations that start small and grow gradually ([Schramm 1992](#); [Peebles 1993](#)). Massive halos, and the galaxies that they contain, assemble from the merger of smaller halos ([Wechsler & Tinker 2018](#)). This hierarchical formation of structure is often depicted as a merger tree ([Somerville & Kolatt 1999](#)). The objects that are giant galaxies today are the products of the assembly of many protogalactic fragments.

There are two basic effects in play: (i) the assembly of mass and (ii) the emergence of an observable, luminous

galaxy through the accretion of gas and its conversion into stars. The timeline of mass assembly (i) is well quantified by N-body simulations ([De Lucia et al. 2006](#); [Srisawat et al. 2013](#)). The second step is highly uncertain, depending on many aspects of gas physics and star formation. However, the luminosity of an individual galaxy cannot outpace its assembly rate ([Naab et al. 2009](#); [van der Wel et al. 2009](#); [Nipoti et al. 2009](#)). Observations of the luminosities of galaxies thus test the predicted formation history.

We describe monolithic and hierarchical galaxy formation models to test with the data in section 2. Constraints on the evolution of high redshift galaxies predating the launch of JWST are discussed in section 3 and new insights from JWST data are examined in section 4. Taken together, the data indicate that structure formed in the early universe at an accelerated pace relative to the predictions of Λ CDM. This result had been anticipated well in advance of the observations ([Sanders 1998](#); [McGaugh 2015](#)) as discussed in section 5. Section 6 provides a succinct summary. We adopt a vanilla Λ CDM universe with $\Omega_m = 0.3$, $\Omega_\Lambda = 0.7$, and $H_0 = 70 \text{ km s}^{-1} \text{ Mpc}^{-1}$ for cosmology-dependent quantities.

2. GALAXY FORMATION MODELS

It is important to have at least two distinct hypotheses to compare and contrast, so we consider both monolithic and hierarchical galaxy formation models. The passive evolution of a monolithic galaxy that forms early is motivated by traditional inferences about the evolutionary history of giant ellipticals (Thomas et al. 2005; Renzini 2006; Bregman et al. 2006; Schombert & Rakos 2009; Schombert 2016). In contrast, hierarchical galaxy formation is expected in Λ CDM (White & Frenk 1991), with testable predictions provided by both semi-analytic galaxy formation models (SAMs) and hydrodynamical simulations. Though something of a straw-man on its own, the monolithic case is useful as a proxy for the predictions (Sanders 1998) of MOND (Milgrom 1983).

2.1. Monolithic Models

An important touchstone in galaxy evolution is the case of the passive evolution of a monolithic island universe (Eggen et al. 1962). The assumption implicit in this hypothesis is that practically all of the mass currently in a galaxy has always been part of it; it evolves as a closed box since a formation redshift z_f . This provides a convenient picture, but is an unrealistic oversimplification. Galaxy-mass balls of gas do not magically appear in the early universe; mass must assemble from the initial condition of a nearly homogeneous early universe (Planck Collaboration et al. 2020). This picture nevertheless provides a useful null hypothesis, and a starting point for more realistic models that assemble mass rapidly if not instantaneously.

2.1.1. Exponential Star Formation History

The growth of the stellar mass of a monolithic galaxy is determined by its star formation history. A common prescription for the passive evolution of a predominantly old stellar population like that of a typical elliptical galaxy (Bregman et al. 2006; Rakos et al. 2008; Schombert & Rakos 2009; Schombert 2016) is an exponential star formation history,

$$\psi(t) = \psi_0 e^{-u}. \quad (1)$$

Here, ψ_0 is a star formation rate that sets the scale that leads to a final mass M_f , and

$$u = \frac{t - t_i}{\tau} \quad (2)$$

where t_i is the time after the Big Bang when star formation begins that we equate to the redshift of galaxy formation z_f , and τ is the timescale over which star formation activity fades. A population can be said to be passively evolving if this timescale is much shorter

than a Hubble time so that most of the stars form in the early universe and evolve passively thereafter. The stellar mass increases as

$$M_*(t) = M_f(1 - e^{-u}). \quad (3)$$

With this prescription for the build-up of stellar mass $M_*(t)$ and the time-redshift relation of vanilla Λ CDM, the luminosity evolution $L(z)$ can be calculated using the methods of stellar population synthesis (Renzini 2006).

Franck & McGaugh (2017) constructed an exponential model with $\tau = 1$ Gyr and a formation redshift $z_f = 10$ corresponding to $t_i = 464$ Myr for vanilla Λ CDM. This was done to provide a baseline against which to compare more realistic models. It was intended as an unrealistic example of a passively evolving galaxy that formed at absurdly high redshift, which $z_f = 10$ was considered to be at the time. Surprisingly, this particular model proved to be the most successful of the many considered by Franck & McGaugh (2017); we refer the reader to this work for other possibilities.

Here, we wish to characterize the evolution of a typical galaxy. To this end, we utilize Schechter (1976) function fits to the luminosity functions of clusters and protocluster candidates (Mancone et al. 2010; Wylezalek et al. 2014; Franck & McGaugh 2017) over a large range of redshifts. We take the characteristic Schechter luminosity L^* to be representative of these populations of galaxies. This enables us to examine the redshift evolution of the corresponding apparent magnitude m^* and stellar mass M_*^* . The virtue of this approach is that it provides a representation of the typical galaxy in an entire galaxy population, not just an individual galaxy, and does so for each cluster at every redshift.

The relation of a model galaxy's luminosity to its stellar mass depends on the adopted initial mass function (IMF) and the details of the population modeling. These are uncertain at the factor of two level, if not more. Here we adopt an empirical calibration by equating the final mass M_f to the characteristic stellar mass $M_*^* = 9 \times 10^{10} M_\odot$ of the Schechter fit to local early type galaxies (Driver et al. 2022) and by matching the corresponding luminosity L^* to the characteristic apparent magnitude m^* of cluster galaxies at $z \approx 1$ (Mancone et al. 2010). This data-informed choice of the mass-to-light ratio is within the range expected for the stellar population models built by Franck & McGaugh (2017): evolutionary theory and data agree at the expected level.

2.1.2. Generalized Star Formation with Quenching

Implicit in the exponential model is the notion that the total baryonic mass of a galaxy assembles promptly

and star formation commences at a high rate instantaneously upon assembly. All of the mass that will become stars by $z = 0$ is present as gas at z_f but forms no stars until t_i when the star formation rate is at its maximum. This is simple conceptually, but obviously naive: stars may form in small clumps (e.g., globular clusters) while the larger quasi-monolithic entity is still in the process of assembling, and gas may continue to accrete and fuel star formation after the bulk of the quasi-monolithic baryonic mass is in place. To improve on this without adding much complexity, we also consider a generalization that allows for a finite ramp-up of star formation before it quenches.

Kelson et al. (2016) show that stochastic star formation leads to an average linear ramp up in the star formation rate $\psi \sim t$ as galaxies accrete gas. This will quickly build up stellar mass as $M_* \sim t^2$. This process is more monolithic than hierarchical, as it envisions in situ star formation from gas accretion onto a single object. Indeed, star formation must quench rapidly in order not to overproduce stellar mass. Regardless of the precise mechanism by which quenching occurs (Peng et al. 2015), an obvious choice to model it is an exponential attenuation with a short e-folding time. Combining this with an initially linear ramp-up gives

$$\psi(u) = \psi_0 u e^{-u} \quad (4)$$

This is only a slight modification to the traditional exponential star formation history described above, providing it with a more realistic initial condition. In principle, we could consider separate timescales for the ramp up of star formation and for its quenching, and could also insert a time delay for the commencement of quenching. We eschew these details for now as unnecessary complications, as we seek only to quantify the approximate time scales relevant to explaining observations of massive galaxies at high redshift. We thus restrict ourselves to the two timescales t_i and τ that are built into the definition of u (eq. 2).

Integrating equation 4, the stellar mass grows as

$$M_*(u) = M_f [1 - (1 + u)e^{-u}] \quad (5)$$

where M_f is the final stellar mass. While no individual galaxy will have exactly this star formation history, eq. 5 provides a simple way to describe the formation and quenching timescales that characterize of a population of galaxies as represented by a typical L^* galaxy.

We shall see that to explain bright galaxies at high redshift (Melia 2023) requires that both the formation time and the e-folding time of quenching be rather short: $\tau \approx t_i \lesssim 0.5$ Gyr, corresponding to formation redshifts

$z_f > 9$. These are obvious candidates to be the progenitors of massive, local galaxies with $M_f \approx M_*^*$ at $z = 0$. That some galaxies have short quenching timescales and evolve into red and dead early type galaxies is not surprising. That such galaxies can form as individual objects that become massive already within the first billion years after the big bang is surprising.

2.2. Hierarchical Models

In contrast to a monolithic model, the hierarchical formation of structure in Λ CDM is a complex combination of in situ growth and growth via merging. The largest galaxies are predicted to form latest, as they take the longest to assemble. That large galaxies are observed to contain the oldest stars (Bregman et al. 2006; Schombert 2016) may thus seem like a contradiction, but it may simply mean that many of the stars formed in protogalaxies at early times prior to them merging into the final giant galaxy (De Lucia et al. 2006; Cattaneo et al. 2008; van der Wel et al. 2009; Nipoti et al. 2009). We thus expect to see many small precursor galaxies at high redshift for every modern giant (Newman et al. 2012; Conselice et al. 2022).

There are many papers in the literature discussing the evolution of galaxies, including theoretical works that attempt to predict how observable galaxies are associated with their parent dark matter halos. While important details vary from model to model (Knebe et al. 2015), the basic prediction of the hierarchical build up of mass is common to all as it is fundamental to the Λ CDM structure formation paradigm. This is well documented by many simulations, for example the IllustrisTNG suite of magnetohydrodynamical simulations (Springel et al. 2018; Pillepich et al. 2018; Marinacci et al. 2018; Naiman et al. 2018; Nelson et al. 2018). Fig. 1 illustrates hierarchical galaxy formation as realized in the high resolution TNG50 simulation (Pillepich et al. 2019; Nelson et al. 2019).

An important aspect of hierarchical galaxy formation is that a massive galaxy at $z = 0$ is the sum of many parts. As we look to high redshift, we do not expect to see an early version of the modern galaxy, but rather its many precursor components. In contrast to a monolithic galaxy, there is no single entity whose evolution we can trace. The closest thing to that is the largest progenitor, which is necessarily smaller at every epoch than the equivalent monolith. For example, a monolith that forms at $z_f = 10$ and evolves with an exponential star formation history with an e-folding time $\tau = 1$ Gyr will form half of its stellar mass by $z = 5$. In contrast, hierarchically assembled galaxies in the Illustris simulation (Rodríguez-Gomez et al. 2016) do not reach this

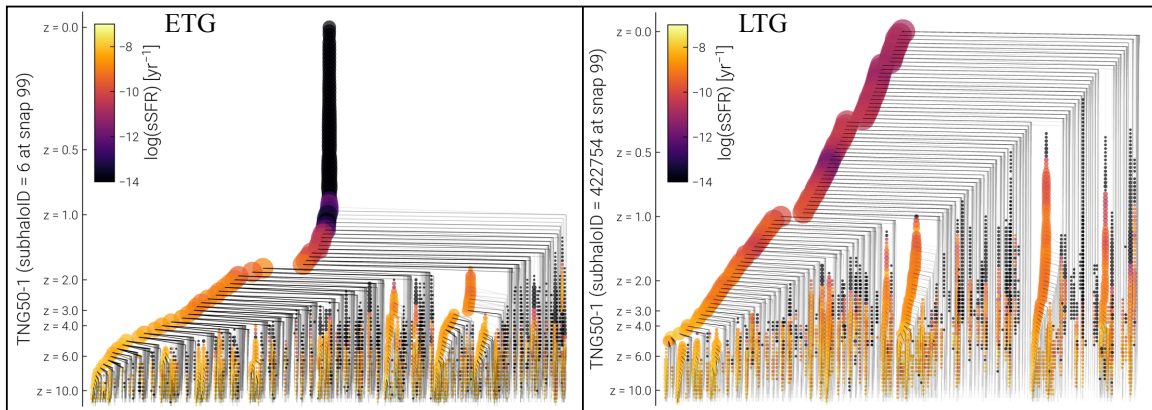


Figure 1. Merger trees for two model galaxies from the TNG50-1 simulation (Pillepich et al. 2019; Nelson et al. 2019) selected to have $M_* \approx 9 \times 10^{10} M_\odot$ at $z = 0$; i.e., the stellar mass of a local L^* early type galaxy (Driver et al. 2022). Mass assembles hierarchically, starting from small halos at high redshift (bottom edge) with the largest progenitor traced along the left of edge each merger tree. The size of the symbol is proportional to the total halo mass and the color bar illustrates the specific star formation rate. A galaxy that quenched long ago is shown at left (labelled ETG); one in which star formation continues to the present epoch is shown at right (LTG).

benchmark until $z \approx 0.7$, taking about half a Hubble time to form half their stars.

The observable light depends on many factors, including the star formation efficiency, the stellar IMF, the mode of gas accretion, and the effects of stellar feedback. These factors provide considerable flexibility to adjust models to account for data, so, as with any theory, the important predictions are those that were made in advance of observation (Mo et al. 1998; Sanders 1998, 2008; McGaugh 2015; Henriques et al. 2015; Rodriguez-Gomez et al. 2016; Anglés-Alcázar et al. 2017; Behroozi & Silk 2018; McGaugh 2022). Whenever possible, it is better to trace the underlying dark mass, the assembly of which is well predicted.

Fig. 1 makes viscerally clear why it is surprising to observe massive galaxies at high redshift. Each present-day L^* galaxy is predicted to be split into a multitude of small progenitors. At $z > 6$, all progenitors are tiny, including the most massive one. This only becomes more severe at $z > 10$. Since it takes a long time to hierarchically assemble the mass necessarily to make an L^* galaxy, it should be possible to distinguish this prediction from the null hypothesis of a monolith in spite of the uncertainties in the details of star formation. Many small objects at $z = 10$ does not look like one big galaxy.

3. HIGH REDSHIFT GALAXIES BEFORE JWST

As we look to high redshift, the first objects we see are always the brightest beacons that have been lit at that time. We must therefore take care to consider how typical these objects are. To do so, we utilize Schechter (1976) function fits to quantify the characteristic stellar mass M_* of large number of galaxies at each redshift. Locally, giant elliptical galaxies have

$M_* = 9 \times 10^{10} h_{70}^{-2} M_\odot$ (Driver et al. 2022). We wish to know the evolution of the *typical* galaxy, $M_*(z)$. Of course, we cannot see the evolution of a single galaxy over cosmic time, and must attempt to infer $M_*(z)$ from snapshots at different redshifts. This is famously problematic, as we can never relate a particular galaxy to its progenitor at higher redshift (Bell et al. 2004). Nevertheless, we can compare the data to evolutionary tracks from models to see which might work and which do not.

The first data from JWST has brought the formation epoch of galaxies and evolution of $M_*(z)$ into sharp focus. While this is a story in progress, it is possible to place these data in the context of precursor work with deep fields observed by HST and Spitzer. Critically, we are not limited to photometric redshifts; there exist many spectroscopic redshifts for many sources (see, e.g., the compilations of Franck & McGaugh 2016a,b).

3.1. Galaxies with Spectroscopic Redshifts

Giant elliptical galaxies are routinely found in dense regions like clusters of galaxies (Dressler et al. 1997) that typically have well-defined red sequences (Bell et al. 2004). This makes clusters and protoclusters convenient environments in which to find a sufficient number of galaxies at the same redshift to construct luminosity functions. This has been done to progressively higher redshifts by Mancone et al. (2010), Wylezalek et al. (2014), and Franck & McGaugh (2017). These studies are all informed by galaxies with spectroscopically observed redshifts, so there is no ambiguity about their cosmic distance as can happen with photometric redshifts. The structures identified as [proto]clusters are redshift spikes in the $N(z)$ diagrams of redshift surveys (Franck & McGaugh 2016a,b), so they represent a pop-

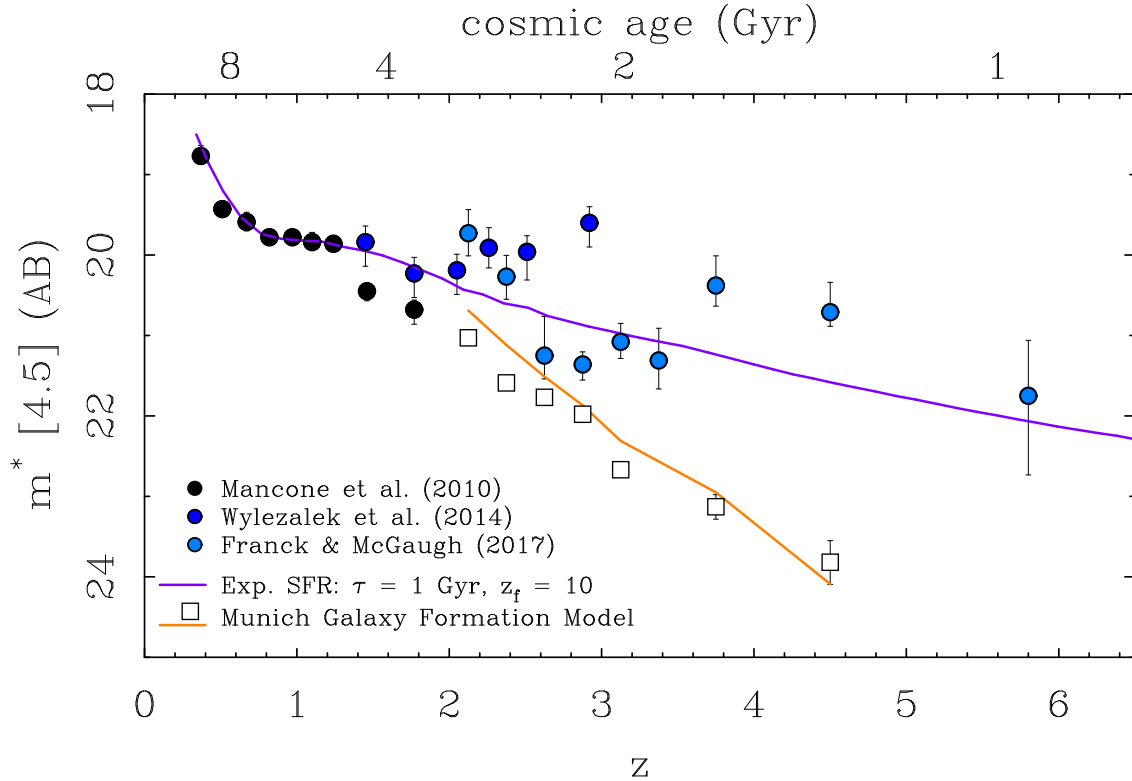


Figure 2. The redshift dependence of the Spitzer [4.5] apparent magnitude m^* of Schechter function fits to populations of galaxies in clusters and candidate protoclusters. Data from Mancone et al. (2010, black circles), Wylezalek et al. (2014, dark blue circles), and Franck & McGaugh (2017, blue circles) all have spectroscopic redshifts. The orange line is the prediction of the Munich galaxy formation model (Henriques et al. 2015) based on the Millennium simulations (Springel et al. 2005; Boylan-Kolchin et al. 2009). Open squares are mock observations of this model using the same algorithm that was applied to the data (Franck & McGaugh 2016a). The predicted characteristic magnitude is fainter than observed, diverging systematically for $z > 2$. The purple line is a model of a galaxy formed at $z_f = 10$ with an exponential star formation history (eq. 1) with $\tau = 1$ Gyr (Franck & McGaugh 2017) normalized at $z \approx 1$. Galaxies like this apparently exist in the high redshift universe, before they were predicted to have assembled, and are common enough to dominate the Schechter fit for m^* .

ulation of galaxies at the same point in the history of the universe regardless of whether they are indeed a bound structure.

Fig. 2 shows the dependence of the AB Spitzer [4.5] apparent magnitude m^* (Franck & McGaugh 2017) corresponding to the characteristic luminosity L^* obtained from Schechter function fits to many dozens, and sometimes hundreds of galaxies in clusters and protocluster candidates. This is a characteristic quantity of the galaxy population, not just a few anecdotal examples. Franck & McGaugh (2017) found no significant difference between the characteristic luminosity of cluster luminosity functions and that of galaxies in the surrounding fields at $z > 2$, so there does not appear to be a strong environment bias at high redshift.

Galaxies become fainter with increasing redshift, as expected (Fig. 2). However, observed galaxies are brighter than anticipated by contemporaneous models, e.g., the Munich galaxy formation model (Henriques

et al. 2015). The model behaves as expected: earlier galaxies are small protogalaxies, so their characteristic luminosity becomes progressively fainter with increasing redshift. This generic expectation of Λ CDM diverges progressively from the data at $z > 2$ (Fig. 2).

As a check that the same quantity was being measured in both data and model, Franck (2018) made mock observations of lightcones from the Munich model (Henriques et al. 2015). The same algorithm was applied to the mock data that was used to identify protocluster candidates in the real data (Franck & McGaugh 2016a,b). The mock observations recover basically the same answer that is known directly from the model (squares in Fig. 2). If the real universe looked like the prediction of the Munich model, we could easily tell. While it is tempting to blame the details of star formation in this particular model, the primary problem is more fundamental. Model galaxies are faint because

hierarchical assembly is incomplete at $z > 3$ (compare Figs. 1 and 2).

In contrast, the data fall around the line representing a monolithic giant that formed at $z_f = 10$ and followed an exponential star formation history (eq. 1). If massive galaxies form early and evolve passively, it would look like the characteristic magnitudes that are observed. In addition to capturing the general trend of the data at high redshift, the data are very well fit at low redshift ($z < 1.5$). This represents passive stellar evolution over most of cosmic time (~ 9 Gyr) after essentially all the stellar mass has been formed and early stochastic variations have had time to subside. These data look very much like the evolution of a massive monolith that was assembled into a single object already at high redshift, and not like Λ CDM models in which the largest progenitor should have been much smaller and fainter at $z > 2$ (Figs. 1 and 2).

As noted in section 2.1.1, no single model line will fit all the data in Fig. 2. The scatter at high redshift presumably reflects stochastic variations in star formation rates at early times (Kelson et al. 2016; Pallottini & Ferrara 2023) before the red sequence was established (Bell et al. 2004; Rakos et al. 2008; Schombert & Rakos 2009; Franck et al. 2015). Nevertheless, the evolutionary trend predicted by the monolithic model captures the essence of the data in a way that the nominal prediction of Λ CDM does not.

3.2. Galaxies at $z > 6$ Before JWST

The bulk of the data discussed above are for $z < 4$ with a couple of candidate protoclusters extending to $z \approx 6$ (Franck & McGaugh 2016b). There have been many studies of galaxies to still higher redshift that pre-date JWST (e.g., Finkelstein 2016; Grazian et al. 2015; Song et al. 2016; Stefanon et al. 2021). These works provide M_* for field galaxies with stellar mass functions measured independently of any of the data described above, albeit at the cost of relying more, if not entirely, on photometric redshifts.

Fig. 3 shows the characteristic stellar mass M_* as a function of redshift. The data from Fig. 2 are shown assuming an exponential star formation history to provide a mapping from magnitude to mass that preserves the distribution of the data. This compares well to the data at higher redshift for which the stellar mass estimates are entirely independent (Finkelstein 2016; Grazian et al. 2015; Song et al. 2016).

We include in Fig. 3 the data of Stefanon et al. (2021) together with those from Fig. 2. This is the most conservative choice in the sense that the stellar mass estimates of Stefanon et al. (2021) are the lowest available at these

redshifts. This happens in large part because Stefanon et al. (2021) make larger corrections for line emission from non-stellar sources. The data are all consistent; they simply attribute less of the observed luminosity to stars.

The data are consistent with a population of massive galaxies that formed early and evolved passively. Despite its naive simplicity, the exponential star formation history (eq. 3 with $\tau = 1$ Gyr) provides a remarkably reasonable depiction of the build up of the characteristic stellar mass seen in Fig. 3. This is highly non-trivial, as the mass build-up happens early while the luminosity evolution is most pronounced at late times (Fig. 2).

More complex star formation histories are admissible. Indeed, stochastic star formation may well drive the scatter seen in the data around $z \approx 3$ when the universe was only ~ 2 Gyr old and stellar populations were necessarily still young. Regardless of the details of the early star formation history, it appears that there exists a population of massive galaxies that formed early and in which most of the stars were made long ago *in a single object* rather than the multiplicity of progenitors envisioned in hierarchical galaxy formation.

Fig. 3 also shows the *a priori* predictions of several Λ CDM models. These include the Munich SAM (Henriques et al. 2015, as in Fig. 2) and the hydrodynamical simulations Illustris (Rodríguez-Gomez et al. 2016) and FIRE (Anglés-Alcázar et al. 2017). These all show basically the same thing. Galaxies are predicted to assemble gradually, with their most massive progenitor not reaching half the final stellar mass until half a Hubble time has passed ($z < 1$). To give a specific example, the Munich SAM reaches half the final stellar mass at $z = 0.68$ when the universe is 7.3 Gyr old. The star formation prescription of FIRE makes more stars earlier, but it is only a small shift of the same basic result: mass assembles too slowly in Λ CDM models. Making star formation more efficient makes more stars earlier, but it does not assemble them into the massive individual galaxies that are observed.

The shortfall of stellar mass in individual galaxies is especially severe at high redshift. At $z \approx 3$, the largest progenitor of an L^* galaxy is only a tenth of its eventual $z = 0$ mass in FIRE. It is even less in Illustris, about 3%. At $z \approx 5$, individual progenitor galaxies are not expected to have grown massive enough to even appear on Fig. 3, let alone to do so at $z \approx 10$. Yet at these redshifts the data show that many galaxies with masses that already approach $M_*(z = 0)$ — enough galaxies to define L^* in a Schechter fit for every point in Fig. 3. This is the normal galaxy population, not just a few extreme individuals. Moreover, spectroscopic redshifts are required to be a

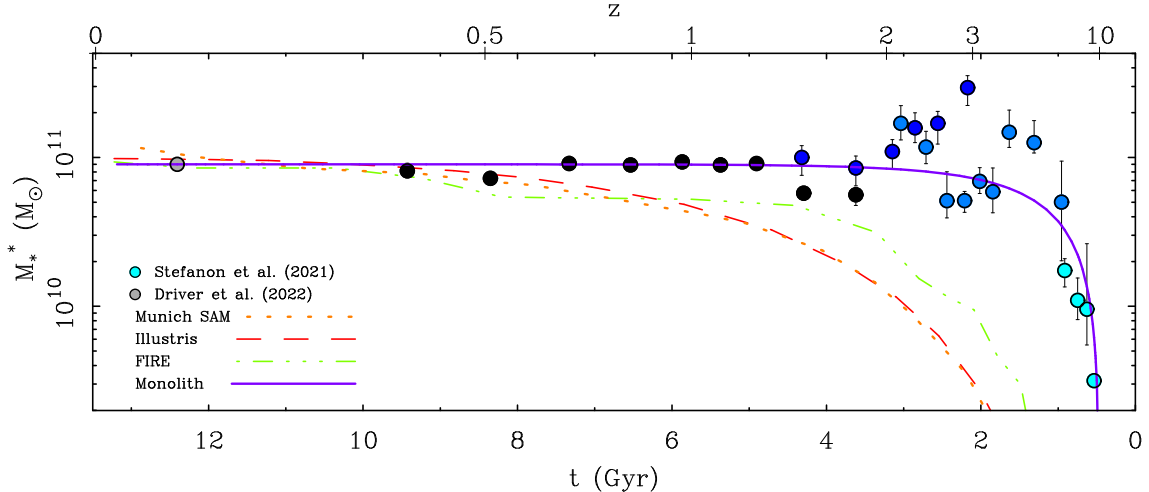


Figure 3. The characteristic stellar mass of the Schechter mass function M_* as a function of time with the corresponding redshift noted at top. The data from Fig. 2 (Mancone et al. 2010; Wylezalek et al. 2014; Franck & McGaugh 2017) are augmented with higher redshift data (Stefanon et al. 2021, light blue points). The purple line is the passively evolving model from Fig. 2 normalized to $M_* = 9 \times 10^{10} M_\odot$ for local elliptical galaxies (Driver et al. 2022, grey point). The dotted orange line shows the build-up of the most massive progenitor of a galaxy that reaches this mass by $z = 0$ in the Munich SAM (Henriques et al. 2015). This is indistinguishable from the result of Illustris (Rodríguez-Gómez et al. 2016, red dashed line). Stellar mass in the FIRE simulation (Anglés-Alcázar et al. 2017, green dot-dash line) grows faster, but only a little.

part of the samples (Franck & McGaugh 2016a,b) that inform the Schechter function fits of Franck & McGaugh (2017), so there is no uncertainty due to photometric redshifts.

3.3. Galaxy Kinematics at Intermediate Redshifts

Kinematic observations provide an independent line of evidence that mature galaxies appeared early in the history of the Universe. Disk galaxies at intermediate redshift ($1 < z < 3$) are observed to have large rotation speeds (Neeleman et al. 2020), to be dynamically cold (Di Teodoro et al. 2016; Lelli et al. 2018, 2023; Rizzo et al. 2023), and to follow scaling relations like Tully-Fisher (Miller et al. 2012; Pelliccia et al. 2017). The Tully-Fisher relation persists up to at least $z \approx 2.5$ when the universe was ~ 2.5 Gyr old (Nestor Shachar et al. 2023). Individual galaxies with high circular speeds and relatively high rotation-to-velocity dispersion ratios are found up to $z \approx 5$ (Rizzo et al. 2020, 2021; Lelli et al. 2021; Roman-Oliveira et al. 2023), barely one billion years after the Big Bang. The early appearance of massive, dynamically cold disks in the first few billion years after the Big Bang is contradictory to both early Λ CDM predictions (Mo et al. 1998, “present-day discs were assembled recently (at $z \leq 1$)”) and the expected hierarchical assembly (Fig. 1) in which early disks are expected to be small and dynamically hot (Dekel & Burkert 2014; Zolotov et al. 2015; Krumholz et al. 2018; Pillepich et al. 2019).

The high rotation speeds observed in early disk galaxies are remarkable. These sometimes exceed 250 (Neeleman et al. 2020) or even 300 km s^{-1} (Nestor Shachar et al. 2023), comparable to the most massive local spirals (Noordermeer et al. 2007; Di Teodoro et al. 2021, 2023). This is important, because the kinematics indicate large dynamical masses for these early galaxies. The problem is not limited to luminosity and the corresponding stellar mass; the underlying dynamical mass is also larger than expected.

The study of kinematics at still higher redshift is a nascent field, but there are already important individual cases. For example, the kinematics of ALESS 073.1 at $z \approx 5$ indicate the presence of a massive stellar bulge as well as a rapidly rotating disk (Lelli et al. 2021). A similar case has been observed at $z \approx 6$ (Tripodi et al. 2023). These kinematic observations indicate the presence of mature, massive disk galaxies well before they were expected to be in place (Pillepich et al. 2019; Wardlow 2021). This is consistent with the ubiquity of disk galaxies in JWST images up to $z \sim 6$ (Ferreira et al. 2022, 2023; Kuhn et al. 2023).

Fig. 4 shows two scaling relations at both low and high redshift: the baryonic mass–circular speed relation (Tully & Fisher 1977; McGaugh et al. 2000) and the dark matter fraction–surface brightness relation (de Blok & McGaugh 1997; Starkman et al. 2018). Both relations are clearly present in the data of Nestor Shachar et al. (2023). Indeed, there is no clear sign of evolution in either relation up to $z \approx 2.5$. The good agreement be-

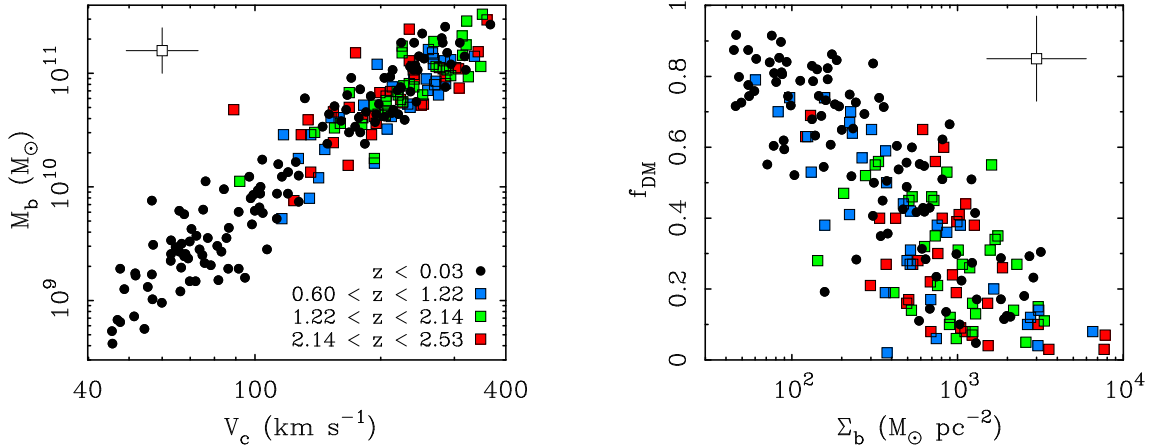


Figure 4. The baryonic Tully-Fisher (left) and dark matter fraction–surface brightness (right) relations. Local galaxy data (circles) are from Lelli et al. (2019) for the Tully-Fisher relation and for spiral disks (Hubble stage $T < 9$) from SPARC Lelli et al. (2016) for the dark matter fraction–surface brightness relation. Higher redshift data (squares) are from Nestor Shachar et al. (2023) in bins with equal numbers of galaxies color coded by redshift: $0.6 < z < 1.22$ (blue), $1.22 < z < 2.14$ (green), and $2.14 < z < 2.53$ (red). Open squares with error bars illustrate the typical uncertainties. The relations known at low redshift also appear at higher redshift with no clear indication of evolution over a lookback time up to 11 Gyr.

tween low and high redshift samples is remarkable given that we have made no attempt to reconcile the precise definition of baryonic mass, which is sensitive to the stellar population model (Schombert et al. 2019), or circular velocity measurement (Lelli et al. 2019). Any systematic differences are apparently within the scatter induced by measurement uncertainties.

The dark matter fraction $f_{DM} = 1 - (V_b/V_c)^2$, where V_c is the observed circular velocity and V_b is that due to the baryons at the same radius. The latter quantity is maximized at 2.2 scale lengths for an exponential disk (Freeman 1970). Many high surface brightness galaxies are maximal disks in which $V_b \rightarrow V_c$ so $f_{DM} \rightarrow 0$ (Starkman et al. 2018) and becomes very sensitive to the stellar population model, which determines the amplitude of V_b . This is less critical for low surface brightness galaxies, which have long been known to be dark matter dominated (de Blok & McGaugh 1997). Fig. 4 shows that the relation between the dark matter fraction and surface brightness was already in place at intermediate redshift (Nestor Shachar et al. 2023) and has not evolved noticeably over cosmic time (Sharma et al. 2023).

Kinematic observations to date show that dynamically cold, massive disks are already present in the universe at early times. These disk galaxies appear to follow the same kinematic scaling relations that are known locally. The presence of dynamically massive galaxies in settled kinematic scaling relations corroborates the ample photometric and spectroscopic data predating JWST (Rocca-Volmerange et al. 2004; Steinhardt et al. 2016; Franck & McGaugh 2017; Merlin et al. 2019) that indicate that galaxies grew too big too fast.

4. HIGH REDSHIFT GALAXIES WITH JWST

JWST has made the observation of galaxies at $z > 10$ seem mundane, so it is worth recalling that this is a recent development. Franck & McGaugh (2017) built the model with $z_f = 10$ shown in Figures 2 and 3 as an extreme upper limit in the context of the widespread presumption at the time that there was no possibility for massive galaxies to have formed that early. Consequently, early JWST results came as a surprise. However, they merely extend the trends already seen in earlier data, corroborating previous indications that galaxies grew too big too fast (e.g., Finkelstein et al. 2022a; Merlin et al. 2022; Melia 2023; Ferrara et al. 2023). While it is early days for JWST, the simple observation is that the high redshift universe contains a bounty of bright, morphologically mature galaxies (Ferreira et al. 2022, 2023) that are more luminous than had been anticipated by Λ CDM models (e.g., Yung et al. 2019a, 2022; Behroozi et al. 2020).

4.1. The UV Luminosity Function

There is a clear excess in the number density of $\sim 10^{10} M_\odot$ galaxies (Stefanon et al. 2021) over the predictions of contemporaneous Λ CDM models (Yung et al. 2019a,b) at $z \approx 8$ (McGaugh 2024). This becomes more challenging to assess at $z > 10$ where much of the observed luminosity is in the ultraviolet where the short-lived nature of high mass stars makes it difficult to assess the corresponding stellar mass. Bearing this caveat in mind, we can nevertheless compare observations (Donnan et al. 2024) and predictions (Yung et al. 2023) (Fig. 5). Again we see a clear excess that is

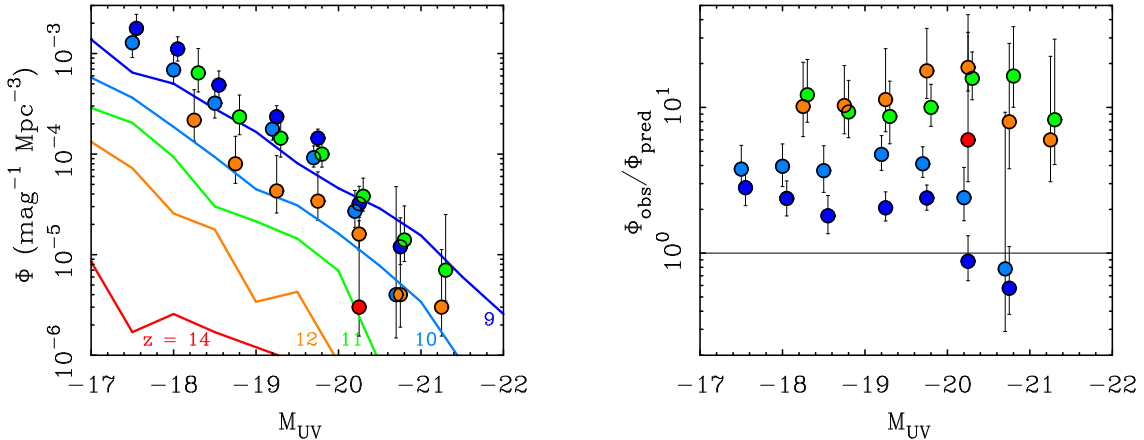


Figure 5. The UV luminosity function (left) observed by Donnan et al. (2024, points) compared to that predicted for Λ CDM by (Yung et al. 2023, lines) as a function of redshift. Lines and points are color coded by redshift, with dark blue, light blue, green, orange, and red corresponding to $z = 9, 10, 11, 12$, and 14 , respectively. There is a clear excess in the number density of galaxies that becomes more pronounced with redshift, ranging from a factor of ~ 2 at $z = 9$ to an order of magnitude at $z \geq 11$ (right).

apparent at all luminosities. Similar results follow from comparison to other predictions (e.g., Behroozi et al. 2020) and other analyses of the observations (Robertson et al. 2023). Λ CDM models did not anticipate the large number of relatively bright galaxies that are observed.

The excess in the number density of UV-bright galaxies is not subtle, being an order of magnitude at $z \geq 11$. This is true despite an upward adjustment of the density in the models by 0.3 to 0.4 dex from Yung et al. (2019a) to Yung et al. (2023). One can imagine a number of ways to further enhance the UV luminosity per unit mass (Finkelstein et al. 2023), but the salient observational fact is that the UV luminosity function barely evolves over the redshift range that the dark matter halo mass function is evolving rapidly. Consequently, any appeal to the efficiency of UV light production must necessarily be fine-tuned to balance the barely-evolving UV luminosity function with the rapidly evolving dark matter halo mass function over a rather small window of cosmic time, there being only $\sim 10^8$ years between $z = 14$ and 11 .

Irrespective of the ultimate interpretation, Fig. 5 clearly illustrates the excess in the number of bright high redshift galaxies over that predicted *a priori*.

4.2. The Mass and Evolution of Individual Galaxies

Despite the clear excess in bright galaxies seen in Fig. 5, it is not yet possible to define a robust population-wide estimate of the corresponding stellar mass M_* as seen in Fig. 3. Nevertheless, there are many individual galaxies (Fig. 6) that have a reasonably persuasive claim to being high mass at high redshift (Adams et al. 2023; Atek et al. 2023; Labbé et al. 2023; Naidu et al. 2022;

Harikane et al. 2023; Finkelstein et al. 2022b; Donnan et al. 2023; Robertson et al. 2023). Most of these are based on photometric redshifts, of which we may reasonably be skeptical. However, it seems unlikely that they are all grossly incorrect given the many independent estimates. Moreover, the essential outstanding feature that they share is how relatively bright they are: galaxies simply do not appear to be as faint as anticipated by Λ CDM models (Fig. 2). Indeed, a change in the photometric redshift (as sometimes happens: Adams et al. 2023) does not necessarily reduce the stellar mass, as a reduction in distance is accompanied by a shift of the flux to bands where the stellar mass-to-light ratio is larger than in the UV. The data discussed by Labbé et al. (2023) are a case in point: all of the initial redshifts and masses were revised downwards after accounting for the on-sky calibration of JWST, but all of them remain problematic in terms of their mass for their redshift. The observational situation will continue to improve as spectroscopic redshifts become available (Wang et al. 2023; Carniani et al. 2024).

Figure 6 shows the stellar masses and redshifts of high redshift galaxies identified in early JWST data (Adams et al. 2023; Atek et al. 2023; Labbé et al. 2023; Naidu et al. 2022; Harikane et al. 2023; Finkelstein et al. 2022b; Donnan et al. 2023; Robertson et al. 2023; Casey et al. 2023; Wang et al. 2023). Unlike Fig. 3, the objects in Fig. 6 are individual galaxies rather than the results of Schechter fits to many. Consequently, they are more plausibly subject to the concern of being rare instances of extreme outliers. However, the masses of these galaxies are very much consistent with a continuation in the trend already seen at intermediate redshift, so the most

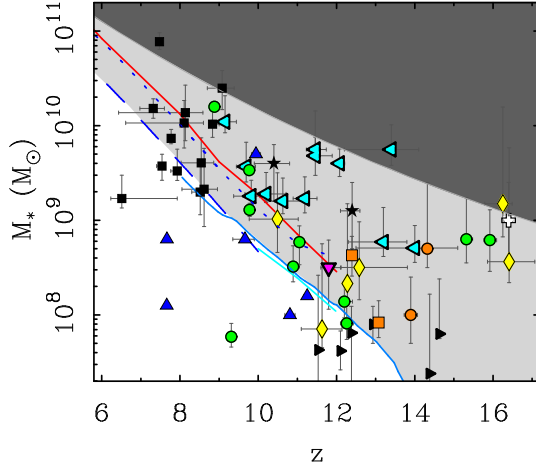


Figure 6. Mass estimates for high redshift galaxies based on JWST data from Adams et al. (2023, dark blue triangles), Atek et al. (2023, green circles), Labbé et al. (2023, squares), Naidu et al. (2022, stars), Harikane et al. (2023, yellow diamonds), Finkelstein et al. (2022b, pink down-pointing triangle), Casey et al. (2023, light blue left-pointing triangles), Donnan et al. (2023, open cross), Robertson et al. (2023, right-pointing triangles), Wang et al. (2023, orange squares) and Carniani et al. (2024, orange circles). The latter two have spectroscopic redshifts. The upper limit for the most massive galaxy in TNG100 (Springel et al. 2018) as assessed by Keller et al. (2023) is shown by the light blue line. This is consistent with the maximum stellar mass expected from the stellar mass–halo mass relation of Behroozi et al. (2020, solid blue line). These merge smoothly into the trend predicted by Yung et al. (2019b) for galaxies with a space density of $10^{-5} \text{ dex}^{-1} \text{ Mpc}^{-3}$ (dashed blue line), though Yung et al. (2023) have revised this upwards by ~ 0.4 dex (dotted blue line). This closely follows the most massive objects in TNG300 (Pillepich et al. 2018, red line). The light grey region represents the parameter space in which galaxies were not expected in Λ CDM. The dark grey area is excluded by the limit on the available baryon mass (Behroozi & Silk 2018; Boylan-Kolchin 2023).

obvious empirical interpretation is that they are indeed typical galaxies. This should become more clear as the sky coverage of deep JWST surveys increases.

A priori Λ CDM predictions for what JWST should see (e.g., Yung et al. 2019b; Behroozi et al. 2020) do not fare well (e.g., Boylan-Kolchin 2023; Keller et al. 2023). The galaxy stellar mass function predicted at high redshift falls precipitously with increasing masses, so Yung et al. (2019b) and Behroozi et al. (2020) anticipate similar limits to the most massive galaxy that should have been seen (Fig. 6). These predictions are corroborated by the analysis of hydrodynamical simulations by Keller et al. (2023), who finds that the locus along which the most massive galaxies should appear. According to Illustris TNG100 (Springel et al. 2018), this locus is essentially

the same as that anticipated by Yung et al. (2019b) and Behroozi et al. (2020). Galaxies should be exceedingly rare to the right of this line, yet appear to be commonplace as assessed by many different observers (Adams et al. 2023; Atek et al. 2023; Labbé et al. 2023; Naidu et al. 2022; Harikane et al. 2023; Finkelstein et al. 2022b; Donnan et al. 2023).

Yung et al. (2023) reassessed their predictions in the light of higher resolution simulations. This results in an upward shift by a factor of ~ 2 (dotted line in Fig. 6). This helps, but only a bit. There remain galaxies of larger mass at higher redshift than should be possible, including examples with spectroscopic redshifts (Wang et al. 2023; Carniani et al. 2024). The space density of such objects remains uncertain: are they typical, or are they merely rare extremes?

It is certainly possible to explain the JWST data with some models. Katz et al. (2023) find a good match of the Sphinx simulation (Rosdahl et al. 2018, 2022) with the cumulative number counts at $9 < z < 13$. In this case, the test may come at lower redshift to which it is not yet computationally feasible to extend Sphinx. Examination of Fig. 34 of Katz et al. (2023) shows the surface density $n(z)$ increasing rapidly with decreasing redshift, implying that this simulation may fit the high redshift data at the risk of overshooting the data at lower redshift (Sabti et al. 2024) as implied by the evolutionary trajectories common in simulations (Fig. 3).

To make our own assessment, we queried the Illustris TNG50 (Pillepich et al. 2019) and TNG300 (Pillepich et al. 2018) simulations to find the most massive model galaxy in terms of stellar mass as a function of redshift. TNG50 has a higher resolution while TNG300 provides a larger box size. Higher resolution helps to see the earliest knots that form, while a large box size contains more rare objects. It is not entirely obvious which of these effects should win out; Yung et al. (2023) find that resolution pushes their estimate up. In the case of the Illustris TNG simulations, box size wins: the objects with the most stellar mass are more massive at every redshift in TNG300 than in TNG 100 than in TNG50. We leave unexamined whether some of these most massive objects might break up if simulated at higher resolution. The TNG300 result closely tracks the estimate of Yung et al. (2023) (red line Fig. 6). Consequently, this line is a conservative estimate of the envelope illustrating a practical upper limit on stellar mass: objects near this line should be exceedingly rare, and nonexistent beyond it.

Observed galaxies populate a region of mass–redshift space where they simply should not be. The assessment of ‘should’ depends on the star formation efficiency, i.e., how effectively nascent dark matter halos convert their

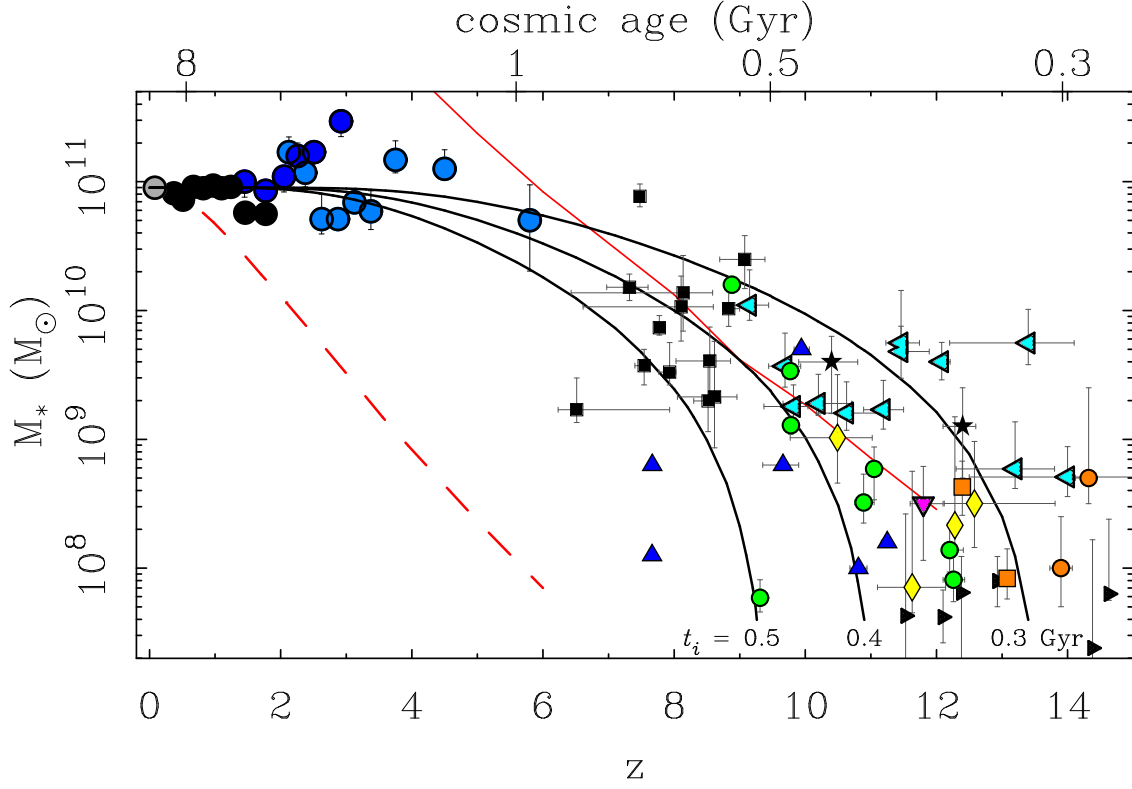


Figure 7. The data from Figures 3 and 6 shown together using the same symbols. The large data points at $z < 6$ represent M_* determined from Schechter fits to many galaxies with spectroscopic redshifts while those at $z > 6$ are individual galaxies observed by JWST. The dashed red line shows the growth predicted by the Illustris Λ CDM simulation (Rodríguez-Gomez et al. 2016) for the typical largest progenitor of a galaxy that reaches a final mass of a typical local ETG ($9 \times 10^{10} M_\odot$; Driver et al. 2022). The solid red line shows the envelope of the most massive objects in TNG300 (Pillepich et al. 2018). The black lines show equation 5 for $M_f = 9 \times 10^{10} M_\odot$ and $t_i = \tau = 0.3, 0.4$, and 0.5 Gyr (top to bottom). Star formation histories like those described by equation 5 are consistent with the illustrated data at all epochs — low, intermediate, and high redshifts — provided that the timescales t_i and τ are both short.

baryons into stars. This can be treated as a free parameter to ease the observed tension; perhaps early-forming halos were more efficient at producing stars. This line of reasoning has a limit, as star formation cannot be more efficient than 100%: there comes a point when dark matter halos lack enough baryons to produce the observed stars (Boylan-Kolchin 2023). A few galaxies appear to challenge this disallowed region (Fig. 6), albeit not many. These may prove illusory (Arrabal Haro et al. 2023), but they are noteworthy as spectroscopic confirmation of truly massive galaxies at these high redshifts would in principle falsify the Λ CDM structure formation paradigm. While it will take some time to assess the severity of this problem, it certainly appears that structure appeared at an accelerated rate in the early universe (Castellano et al. 2022, 2023).

Fig. 7 combines the data from Figures 3 and 6 to show the stellar mass of galaxies observed over all of accessible cosmic time. Also illustrated are the generalized star formation history (eq. 5) and that from Illustris

(Rodríguez-Gomez et al. 2016) and TNG300 Pillepich et al. (2018). Illustris illustrates the stellar mass growth of the largest progenitor of a typical galaxy that attains a final mass consistent with M_* for local early type galaxies (Driver et al. 2022). TNG300 illustrates the most massive model galaxy in that simulation. These parallel one another; other Λ CDM models and simulations follow a similar trajectory with modest variations (Fig. 3). These variations stem from differences in the implementation of baryonic physics, not the assembly of mass (Fig. 1).

The most massive progenitors of typical galaxies in Λ CDM models fall well short of the data as a function of redshift. This discrepancy is already perceptible at $z = 1$, clear at $z = 2$, and glaring for $z > 4$. We can imagine that the anecdotal examples of bright individual galaxies found in early JWST data at $z > 8$ are early adopters, being the brightest beacons that form first and are the most visible, things like the most massive objects in TNG300. However, the data do not appear to follow

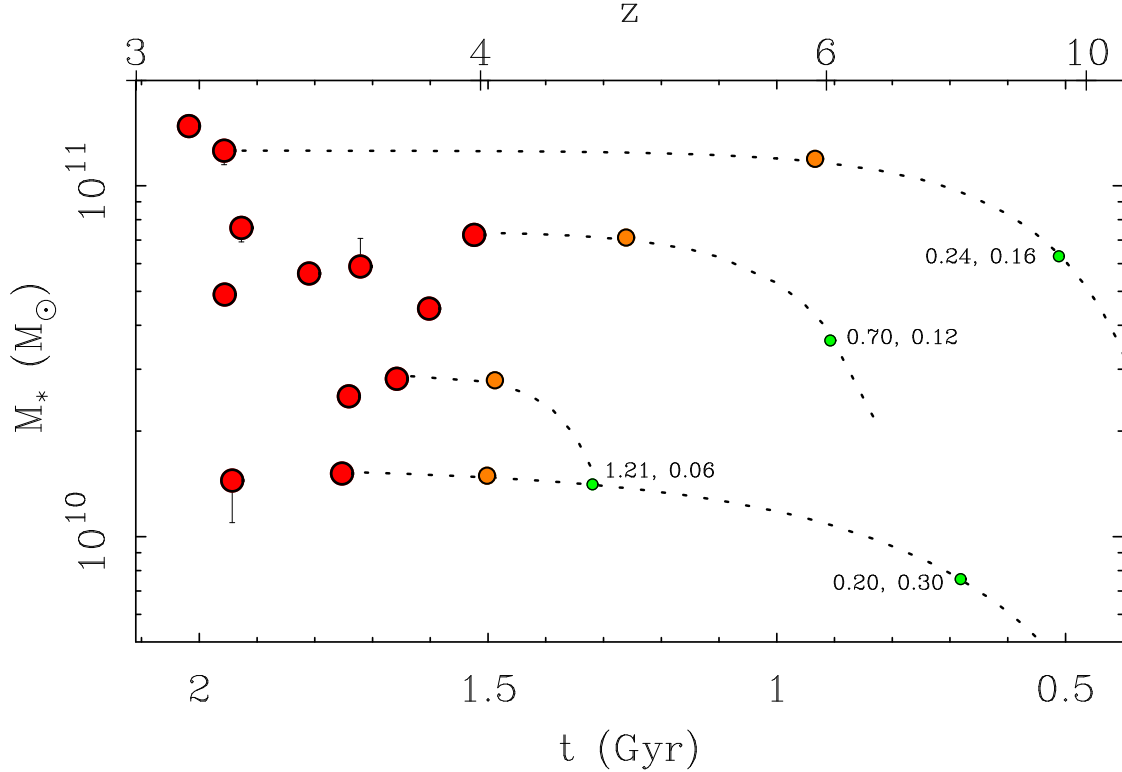


Figure 8. The stellar masses of quiescent galaxies from Nanayakkara et al. (2024). The inferred growth of stellar mass is shown for several cases, marking the time when half the stars were present (small green circles) to the quenching time (mid-size orange circles) to the epoch of observation (large red circles). Illustrative star formation histories following equation 5 are shown as dotted lines with parameters t_i, τ in Gyr noted. We omit the remaining lines for clarity, as many cross. There is a wide distribution of formation times from very early ($t_i = 0.2$ Gyr) to relatively late (> 1 Gyr), but all of the galaxies in this sample are inferred to build their stellar mass rapidly and quench early ($\tau < 0.5$ Gyr).

the predicted linear track of growth, and would grow too massive by low redshift if they did so.

Fig. 7 also illustrates evolutionary tracks for the generalized star formation history encapsulated by eq. 4. These naturally encompass both high and low redshift data, and better resemble the distribution of the data than do the approximately linear tracks of Λ CDM models. The available data suggest that there exists a population of galaxies for which both the formation and quenching timescales are short: $t_i \approx \tau \lesssim 0.5$ Gyr. Such an evolutionary history is consistent with the traditional picture of a monolithic giant elliptical galaxy.

The problem for Λ CDM is perhaps most severe at intermediate redshifts where the luminosity functions of entire populations of galaxies have been measured, not just a few anecdotal cases. At $z \approx 3$, the universe is only ~ 2 Gyr old (a lookback time in excess of 11 Gyr), but galaxies with $M_* > 5 \times 10^{10} M_\odot$ are already commonplace. At this time, the typical massive galaxy is predicted by Λ CDM (Rodríguez-Gomez et al. 2016) to have assembled an order of magnitude fewer stars. This discrepancy is not subtle, nor can it be explained away

by photometric redshifts or top-heavy IMFs. The relevant observations are based on spectroscopic redshifts, and the stellar masses are robust, having been derived from observations of rest-frame optical and near-infrared emission rather than the rest frame ultraviolet. These data point to galaxies having grown too big too fast.

4.3. Quenched Galaxies

Another important observation is that of quenched galaxies at $3 < z < 4$ (Schreiber et al. 2018; Merlin et al. 2019; Nanayakkara et al. 2024; Glazebrook et al. 2023). These galaxies have observed spectra that show the classic features of a stellar population aging after intense star formation at an earlier epoch. Not only do massive galaxies exist by $z \approx 4$, but there are examples that have stellar populations that are old for the age of the universe at the redshift of observation. By modeling the observed spectra, it is possible to estimate the stellar mass at the time of quenching and roughly when half the stellar mass was in place in addition to the mass at the observed redshift. This provides an approximate curve of growth for each galaxy, as illustrated in Fig. 8.

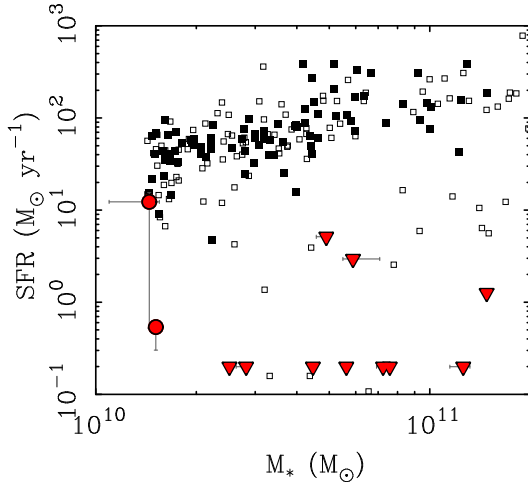


Figure 9. The stellar masses and star formation rates of galaxies from Nanayakkara et al. (2024, red symbols). Downward pointing triangles are upper limits; some of these fall well below the edge of the plot so are illustrated as the line of points along the bottom. Also shown are objects selected from the TNG50 (Pillepich et al. 2019, solid squares) and TNG300 (Pillepich et al. 2018, open squares) simulations at $z = 3$ to cover the same range of stellar mass. Simulated objects with stellar masses comparable to real galaxies are mostly forming stars at a rapid pace. In the higher resolution TNG50, none have quenched as observed.

The growth rates inferred by Nanayakkara et al. (2024) are consistent with the rapid rate of growth illustrated by the monolithic model (eq. 5). Individual galaxies vary in mass, but all are consistent with following a similar evolutionary trajectory. Further examples of such galaxies at still higher redshift are discussed by Wang et al. (2024). These galaxies grew too big too fast, well ahead of the expectation in Λ CDM models.

Galaxies that formed most of their stars early and then quenched is consistent with the traditional view of the evolution of monolithic early type galaxies. That the galaxies observed by Nanayakkara et al. (2024) have masses consistent with other high redshift galaxies and show the evolved spectra expected for stellar populations descended from earlier star formation suggests that the most obvious interpretation of the data is also the most likely: bright galaxies at high redshift are intrinsically luminous because they contain lots of stars. They apparently formed as giant monoliths at early times.

The depiction of evolutionary tracks in Fig. 8 implicitly assumes all the mass was assembled at an early time. It is also conceivable that the galaxies observed by Nanayakkara et al. (2024) at $z \approx 3$ to 4 were not individual objects at the time of quenching or when half the stellar mass had formed. These events could in-

stead have occurred in protogalactic fragments that subsequently merged to form the observed galaxies. Since the assembled stars are old for the epoch of observation, the assembly must occur as dry mergers devoid of star formation: the stars must be made first in protogalactic chunks (Newman et al. 2012; Conselice et al. 2022). To check what Λ CDM predicts, we have searched the TNG50 and TNG300 simulations (Nelson et al. 2018, 2019) for model galaxies at $z = 3$ with stellar masses in the same range as the data of Nanayakkara et al. (2024). Many examples of such objects exist in the simulations, but almost all are actively star forming (Fig. 9). Quenched galaxies are rare in the simulations at this redshift, with all branches of the merger trees experiencing high specific star formation rates at $z > 3$ (Fig. 1). So while it is possible to find simulated objects of the observed stellar mass, their star formation histories are not a good match to those observed.

It is difficult to avoid the conclusion that observations of the high redshift universe are genuinely problematic for Λ CDM (Haslbauer et al. 2022b). The early appearance of massive galaxies was already apparent in spectroscopic data (Fig. 2) predating the launch of JWST (Steinhardt et al. 2016; Franck & McGaugh 2017). These galaxies are not exceptional individuals, but rather are typical at intermediate redshifts (Fig. 3). The remarkable discoveries being made by JWST corroborate and extend this result (Adams et al. 2023; Atek et al. 2023; Labbé et al. 2023; Naidu et al. 2022; Harikane et al. 2023; Finkelstein et al. 2022b; Donnan et al. 2023; Nanayakkara et al. 2024). Many lines of evidence indicate that there exists a population of exceptionally high mass galaxies in the early universe, galaxies that from the perspective of Λ CDM grew too big too fast.

5. ACCELERATED STRUCTURE FORMATION

The discussion to this point has been within the conventional Λ CDM framework, for which the results are anomalous. A natural question is how such anomalies might arise. That structure could and *should* form at an accelerated pace was anticipated well in advance by Sanders (1998), McGaugh (1999a), Stachiewicz & Kutschera (2001), Sanders (2008), and others — see McGaugh (2015) and references therein. The new physics driving the prediction of early structure formation is MOND (Milgrom 1983). MOND has a lengthy track record of predictive success (Milgrom 2014), many aspects of which are not satisfactorily explained by dark matter (McGaugh 2020). The early formation of massive galaxies is another predictive success.

5.1. Cosmic Context

MOND has been very successful as a theory of galaxy dynamics (Sanders & McGaugh 2002; Famaey & McGaugh 2012; Banik & Zhao 2022), but has no completely satisfactory cosmology (Wittenburg et al. 2023). We need a deeper theory that encompasses both MOND and General Relativity. No completely satisfactory deeper theory yet exists (Famaey & McGaugh 2012) just as no laboratory detection of dark matter has been obtained.

Perhaps the most successful attempt to combine MOND and General Relativity to date is the Aether-Scalar-Tensor (AeST) theory of Skordis & Złóśnik (2019). AeST has been shown to fit the power spectrum of both the cosmic microwave background and galaxies at low redshift (Skordis & Złóśnik 2021), but many details of the theory remain to be explored. One possible shortcoming is an apparent tension between the parameters required to explain the data at small, intermediate, and large scales (Mistele et al. 2023).

In this context, it is worth remembering that Λ CDM works if and only if some form of invisible non-baryonic mass genuinely exists despite the persistent laboratory non-detection of the expected candidate particles. From this perspective, dark matter and dark energy may just be inferences made to approximate a deeper theory absent the knowledge thereof. While the deeper theory remains unknown, we know the universe is expanding, and that MOND often works to describe the dynamics of objects within it. In what follows, we simply consider what happens to a region within the expanding universe that is subject to the MOND force law.

5.2. Structure Formation in MOND

MOND is inherently nonlinear. The $\sim 10^5$ growth factor from $z = 1090$ to $z = 0$ is achieved through nonlinear growth (Nusser 2002; Knebe & Gibson 2004; Llinares et al. 2008) rather than linear growth with cold dark matter. Indeed, the usual linear growth rate cannot reconcile the new JWST results with previous results from HST (Sabti et al. 2024): the data themselves indicate nonlinearity.

Calculating the nonlinear growth of structure in MOND is a nontrivial problem (Sanders 1998; Stachiewicz & Kutschera 2001; Sanders 2001; Nusser 2002; McGaugh 2004; Llinares et al. 2008; Feix 2016; Wittenburg et al. 2020) and considerable work remains to be done. Nevertheless, a common feature of these analyses is a rapid period of structure formation. Indeed, this seems unavoidable when considering a MONDian region within an expanding background.

Sanders (1998) considered spherical regions in the MOND regime in an expanding Universe. After first showing that the usual early universe results (e.g.,

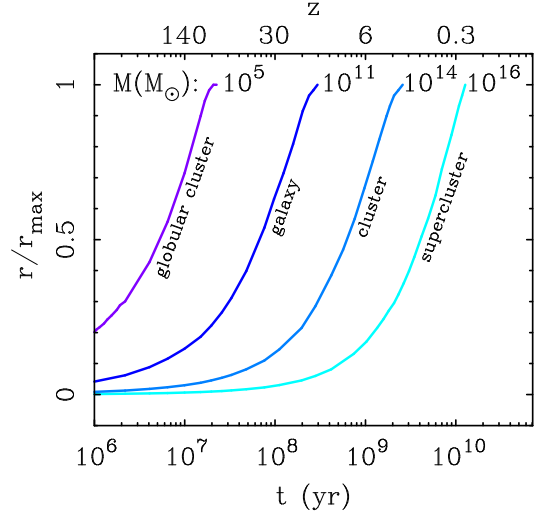


Figure 10. The expansion of spherical regions of various masses in MOND as a function of time (Sanders 1998). Globular clusters collapse first and form early. Large galaxies reach maximum expansion after $\sim 3 \times 10^8$ yr; rich clusters of galaxies do so after $\sim 3 \times 10^9$ yr. Laniakea (Tully et al. 2014) and Ho’oleilana (Tully et al. 2023) may be examples of vast structures near turnaround today. The redshift scale on the top axis assumes vanilla Λ CDM for reference, but the time–redshift relation may differ in MOND.

Big Bang Nucleosynthesis) are retained, Sanders (1998) showed that there is a characteristic length scale r_c below which MOND dynamics should apply. The value of r_c grows with time, with small regions entering the MOND regime first and larger ones later in a hierarchical sequence, albeit one greatly accelerated relative to Λ CDM. On scales larger than r_c , the Universe remains homogeneous and isotropic, so the conventional Friedmann equation may continue to apply. On scales smaller than r_c , the region becomes detached from the Hubble expansion and is destined to recollapse under its own gravity. This process is inevitably inefficient: not all regions of the universe will be neat spheres that are cleanly in the MOND regime. Those which are must necessarily collapse rapidly, so there should be a portion of the galaxy population that forms early.

The governing equation for an initially expanding spherical region in the MOND regime (Felten 1984; Sanders 1998) is

$$(\dot{r})^2 = (\dot{r}_i)^2 - \left(\frac{16\pi}{3} a_0 G \rho_b r_0^3 \right)^{1/2} \ln(r/r_i), \quad (6)$$

where r_0 is the comoving radius of the spherical region, r_i and \dot{r}_i are the initial radius and expansion velocity thereof, ρ_b is the baryonic mass density, and $a_0 = 1.2 \times 10^{-10} \text{ m s}^{-2}$ (Begeman et al. 1991; McGaugh et al. 2016). The introduction of the dimensional

constant a_0 makes the problem scale-dependent (Felten 1984), so the initial conditions matter. Fortunately, r_i and \dot{r}_i have an obvious interpretation: since this growth can only commence after radiation releases its grip on the baryons, the initial velocity is simply the cosmic expansion rate at that time while the initial radius specifies the mass of the object. The precise redshift when this occurs is sensitive to the cosmology (Sanders 1998), but happens early enough ($z \gtrsim 200$) that the net result for galaxy mass objects is not particularly sensitive to the initial conditions: the start time is small compared to the subsequent evolution. A region that evolves according to eq. 6 reaches a mass-dependent maximum radius and recollapses on a timescale comparable to that of the initial expansion (Fig. 10).

5.3. The Early Formation of Massive Galaxies

The early formation of massive galaxies was explicitly predicted by Sanders (1998): “Objects of galaxy mass are the first virialized objects to form (by $z = 10$), and larger structure develops rapidly.” Contrast this with the contemporaneous Λ CDM statement by Mo et al. (1998): “present-day discs were assembled recently (at $z \leq 1$).” One of these *a priori* predictions is consistent with the data.

Since the background cosmology remains unknown in MOND, the time–redshift relation is not firmly established. The predictions of Sanders (1998) are based on the dynamical evolution of a spherical top-hat embedded in an expanding universe. In a pure MOND universe, such a region is destined to recollapse (Felten 1984) irrespective of its initial density (eq. 6), with small regions naturally collapsing faster than large ones. The mass of the top-hat sets the timescale for decoupling from the Hubble flow (Sanders 1998) and recollapse (Stachniewicz & Kutschera 2001). This predicted timescale is more fundamental than the corresponding redshift, which is cosmology-dependent (Clifton et al. 2012; Skordis & Złótnik 2021). Hydrodynamics is important at the scale of globular clusters, which briefly delays their collapse (Stachniewicz & Kutschera 2001). It is less important at galaxy scales, collapse is approximately symmetric with the expansion illustrated in Fig. 10.

The salient prediction Sanders (1998) made is that “Massive galaxies ($10^{11} M_\odot$) reach the point of maximum expansion at $t = 3 \times 10^8$ years.” Collapse happens in a similar time for objects of this mass (Stachniewicz & Kutschera 2001), so in principle a massive protogalaxy can be assembled in 600 Myr. Wittenburg et al. (2020) consider slightly lower mass objects, and find that “after approximately 0.5 Gyr the spheres collapse and form a rotating dense, thin disk.” This is the timescale for

forming galaxies in MOND. This corresponds to $z \approx 8$ in Λ CDM, and still higher redshift in the low density, baryon-only FLRW cosmologies considered by Sanders (1998) (see also Stachniewicz & Kutschera 2001; Sanders 2001; McGaugh 2004; Sanders 2008; Llinares et al. 2008; McGaugh 2018).

Globular cluster mass ($\sim 10^5 M_\odot$) objects collapse very quickly, in a few tens of millions of years (Stachniewicz & Kutschera 2001). This is so fast that they will have ages that are practically indistinguishable from that of the universe itself (Ying et al. 2023). A large range of masses can collapse within the first Gigayear: this is the epoch of galaxy formation in MOND. This provides a natural explanation for the remarkably early formation times t_i inferred in Fig. 7. Structure formation is hierarchical insofar as globular clusters form more quickly than massive galaxies, but the pace is accelerated to the point that it appears nearly monolithic after many billions of years.

5.4. Larger Structures

Accelerated formation applies to all structure in MOND, not just individual galaxies. Larger structures like massive clusters of galaxies should also form earlier than in Λ CDM. Indeed, the entire cosmic web should emerge earlier (McGaugh 2015), and should be perceptible in the distribution of high redshift quasars. Indications to this effect already exist (e.g., Shen et al. 2007; Eilers et al. 2024; Pizzati et al. 2024).

A region destined to become a cluster of galaxies will reach maximum expansion after 2 – 3 Gyr (Sanders 1998), so clusters should also emerge as recognizable objects fairly early in the development of the universe, and certainly earlier than anticipated in Λ CDM where they are the last bound structures to form. Kravtsov & Borgani (2012) show that a $\sim 10^{15} M_\odot$ cluster is barely getting started at $z = 3$ (see their Fig. 6). Note that in MOND there is no cold dark matter, so the equivalently massive clusters is of order $10^{14} M_\odot$. Sanders (1998) predicts “that by $z = 3$ not only do massive galaxies exist but they are also significantly clustered (the density of the $10^{14} M_\odot$ region would be enhanced by a factor of 6.5 over the mean at this redshift).”

Franck & McGaugh (2016a,b) identify dozens of protocluster candidates at redshifts $2 < z < 6.6$ (Fig. 11). Of these, the sixteen most reliable candidates have $N \geq 10$ spectroscopically confirmed members with overdensities ranging from 5 to 20 with a median $\delta = 9.5$. Similar structures have recently been identified by Shah et al. (2024), including six massive protoclusters around $z \approx 3$. This is consistent with the findings of Franck & McGaugh (2016b) and the predictions of MOND, but

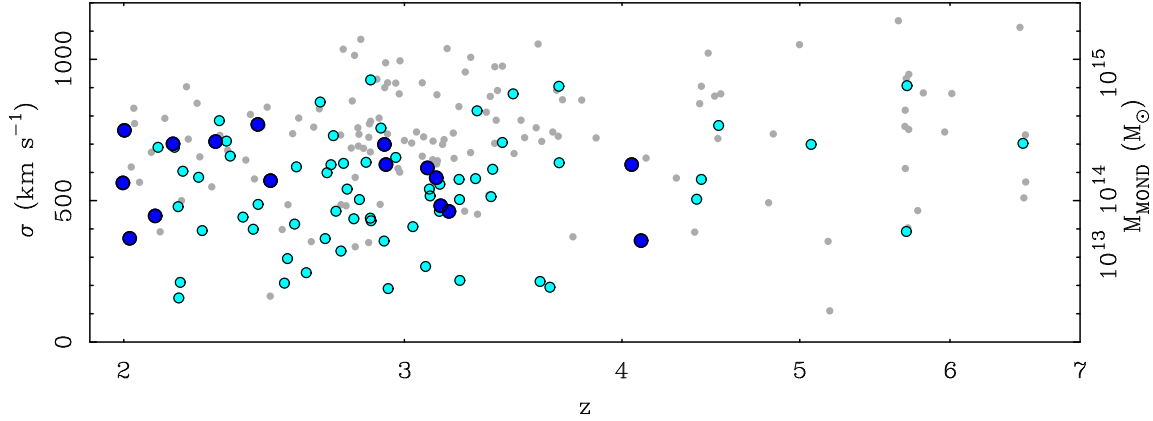


Figure 11. Measured velocity dispersions of protocluster candidates (Franck & McGaugh 2016a,b) as a function of redshift. Point size grows with the assessed probability that the identified overdensities correspond to a real structure: all objects are shown as small points, candidates with $P > 50\%$ are shown as light blue mid-size points, and the large dark blue points meet this criterion and additionally have at least ten spectroscopically confirmed members. The MOND mass for an equilibrium system in the low acceleration regime is noted at right; these are comparable to cluster masses at low redshift.

rather higher than expected in Λ CDM (Kravtsov & Borgani 2012; Mortonson et al. 2011).

A number of the best candidate clusters of Franck & McGaugh (2016a,b) are at $z \sim 3$. The median velocity dispersion of candidate clusters is $\sim 600 \text{ km s}^{-1}$ (Fig. 11). This is about twice that of equivalent systems found in lookback cones in Λ CDM simulations (Franck 2018). That is, protocluster candidates identified as spikes in $N(z)$ have larger velocity dispersions in the data than in simulations at the same redshift. This is another indication that the discrepancy is one in mass, not just luminosity. These systems should not yet be bound in Λ CDM, but it is possible that they have already formed in MOND (Fig. 10).

The median observed velocity dispersion of intermediate redshift cluster candidates corresponds to a mass of $\sim 10^{14} M_{\odot}$ for systems in dynamical equilibrium in the deep MOND regime (Milgrom 2018, 2019, 2021). These numbers are very much in line with the long-standing prediction of Sanders (1998), and are similar to the masses inferred for clusters in MOND at low redshift (McGaugh 2015; Li et al. 2023; Tian et al. 2024). Galaxy clusters are known to display a residual mass discrepancy in MOND of about a factor of two (Sanders 2003, 2007; Angus et al. 2008), so there is an apparent need for an extra mass component, possibly in the form of undetected baryons (Milgrom 2008; Kelleher & Lelli 2024). We are thus in the curious situation that the masses of galaxy clusters remain problematic for MOND at the factor of two level, but their formation time is potentially problematic for Λ CDM, as are other properties like cluster collision speeds (Angus & McGaugh 2008; Katz et al. 2013) and the largest mass objects (Asencio et al. 2021).

Sanders (1998) notes that the largest structures nearing turnaround today would be superclusters (Sankhyayan et al. 2023). These are not expected to be simple objects, as they are inevitably far from the simple spherical approximation of eq. 6. Indeed, it was recognized early (Felten 1984) that MOND would induce anisotropy on unexpectedly large scales. These considerations anticipate the size and complex kinematics of objects like Laniakea (Tully et al. 2014) and Ho’oleilana (Tully et al. 2023), and motivate searches for anisotropy in the expansion rate.

5.5. Other Indications

The morphology of cosmic structure is similar in Λ CDM and MOND (Llinares et al. 2008; McGaugh 2015), but accelerated structure formation of MOND pushes all benchmarks for structure formation to earlier times in cosmic history. The cosmic web emerges early, providing a natural explanation for the clustering of high-redshift quasars (Clowes et al. 2013) and other very large features (Horváth et al. 2014, 2015; Balázs et al. 2015; Lopez et al. 2022). Indeed, one can see indications of the clustering of protoclusters at high redshift (Franck & McGaugh 2016b), which is visible in Fig. 11 as the multiplicity of objects at similar redshift. These features are larger than expected in Λ CDM, but quite natural in MOND. MOND is also effective (Llinares et al. 2008; McGaugh 2015) at making large, empty voids (Nusser et al. 2005; Peebles & Nusser 2010).

At still higher redshift, other natural consequences of early structure formation include early reionization (McGaugh 1999b) and an enhanced ISW effect (McGaugh 2004), for which there is some evidence (Granett et al. 2008; Nadathur et al. 2012; Kovács et al. 2020). Predic-

tions for 21 cm absorption at cosmic dawn and during the dark ages are discussed by [McGaugh \(2018\)](#). The depth of the absorption signal can be deeper than in Λ CDM at both epochs ($z \approx 17$ and $z \approx 100$). Due to the nonlinear growth of structure, one expects less power in fluctuations entering the dark ages ($z \sim 150$) but more by their end ($z \sim 50$) than in Λ CDM. This is the epoch when the seeds of structure planted by MOND begin to sprout.

At late times, it becomes difficult for a MOND universe to remain isotropic ([Felten 1984](#)). This would go some way to explain the tension between the dipole anisotropy of number counts of distant sources and the cosmic microwave background ([Secrest et al. 2021, 2022; Domènech et al. 2022](#)) and perhaps lead to an anisotropy in cosmic expansion ([Colin et al. 2019](#)). It seems that many of the puzzling observations in cosmology may be attributed to MOND. Indeed, many of these things were predicted *a priori*.

6. SUMMARY

We have examined evidence concerning the evolution of galaxies across a large range of redshifts for which data are available. There appears to be a population of bright galaxies that formed early and grew rapidly. There is copious photometric evidence that indicates the existence of this population, and important corroborative evidence from kinematics.

6.1. Photometric Evidence

The galaxy population that grew too big too fast has photometric properties that suggest it is

- luminous, with apparent magnitudes considerably brighter than anticipated by contemporaneous Λ CDM models (Fig. 2);
- massive, with typical examples approaching the mass of a local L^* galaxy already by $z \approx 3$ when the universe was only ~ 2 Gyr old (Fig. 3);
- old, with stellar populations consistent with forming at high redshift $z_f \gtrsim 10$ (Figs. 7 and 8) and quenching early (Fig. 9);
- common in clusters at $z \lesssim 3$ and already clustered in protoclusters at $z \lesssim 6$ (Fig. 11); and
- consistent with the population of bright galaxies observed by JWST at $z > 10$ (Fig. 7) where bright galaxies are more common than anticipated (Figs. 5 and 6).

These observed properties do not sit well with the predictions of hierarchical Λ CDM models, which predict

that local massive galaxies were divided into many progenitor protogalaxies at the observed redshifts (Fig. 1). They are instead consistent with a population of galaxies that formed early as massive quasi-monoliths, i.e., the traditional picture of giant elliptical galaxies that form early and quench rapidly, following something like an exponential star formation history (Figs. 2 and 3).

Λ CDM galaxy formation models failed to anticipate the bright galaxies that are observed at both intermediate and high redshift. Forming enough stars is not the problem. The problem is assembling them into a single object. The presence of these quasi-monolithic objects appears to violate the hierarchical assembly paradigm (Fig. 1).

Since there is little flexibility to adjust the mass assembly history in Λ CDM, one might instead consider adjusting the efficiency of early star formation, thus making small mass protogalaxies brighter than nominally expected. This may be a viable approach at $z > 10$, but does not provide a satisfactory explanation for the bright galaxies observed at intermediate redshift ($2 < z < 6$). These objects have spectroscopic redshifts and good multi-band photometry covering the rest frame optical portion of the spectrum, so neither their cosmic distances nor their stellar masses can be sufficiently in error as to explain the large discrepancy. Moreover, they are common enough to define a value for L^* that is much brighter than the predictions of Λ CDM models ([Steinhardt et al. 2016; Franck & McGaugh 2017](#)).

The observation of bright galaxies by JWST at still higher redshifts, $z > 10$, came as a surprise because that is clearly not what Λ CDM predicts (Fig. 1). This high redshift problem seems more tenable than that at intermediate redshift since we are more reliant on photometric redshifts and UV luminosities that are notoriously difficult to relate to stellar mass. Though this leaves room for flexibility in modeling, the observed UV luminosity function hardly evolves at $z \gtrsim 10$ where the dark matter halo mass function should be evolving rapidly (Fig. 5). In order to explain the data by adjusting the efficiency of star formation or UV light production, there must be a fine-tuning to reconcile these very different evolutionary behaviors over a small portion of cosmic time ($< 2 \times 10^8$ Myr).

A more natural interpretation is that galaxies are bright at high redshift because they had already grown large. This provides an evolutionary trajectory that maps nicely between observations at low, intermediate, and high redshift. Note that it is not necessary for all galaxies to form early and follow such a trajectory, just enough of them to define a bright L^* in early ($z \approx 3$) clusters ([Franck & McGaugh 2017](#)). This population

was not anticipated by Λ CDM models and is not easily reconciled with them: these galaxies grew too big too fast.

The discrepancy between the stellar masses of intermediate and high redshift galaxies and the prediction of Λ CDM is not subtle: galaxies became too big too fast by a large factor. It is common to see galaxies at $z \approx 3$ (when the universe was ~ 2 Gyr old) that have a stellar mass that is already approaching that of L^* galaxies at $z = 0$. In contrast, Λ CDM models consistently predict that the largest progenitor of such galaxies should have a rather smaller fraction of their final stellar mass in place at this early time (Fig. 3): FIRE (Anglés-Alcázar et al. 2017) predicts $\sim 10\%$, Illustris $\sim 3\%$ (Henriques et al. 2015; Rodríguez-Gomez et al. 2016). This poses a challenge to the assembly history of mass in the Λ CDM structure formation paradigm, not just the evolution of the luminous component.

6.2. Kinematic Evidence

Photometric observations are complemented by kinematic observations that trace the mass, not just the light. JWST observations show that morphologically mature spiral galaxies are common at early times (Ferreira et al. 2022, 2023). Kinematic observations to date (section 3.3) show that rotationally supported galaxies

- formed early, by $z \gtrsim 6$ (Smit et al. 2018; Rowland et al. 2024; Xu et al. 2024) when $z \leq 1$ had been the nominal expectation (Mo et al. 1998);
- rotate fast, with circular speeds in excess of 250 km s^{-1} (Rizzo et al. 2021; Lelli et al. 2021), comparable to massive local spirals;
- obey the Baryonic Tully-Fisher relation (Lelli et al. 2019; Nestor Shachar et al. 2023); and
- obey the dark matter fraction–surface brightness relation (Fig. 4).

These observations show that at least some spiral galaxies formed early and became massive rapidly. Note that kinematic observations imply a large dynamical mass: it is not just a matter of stars producing more light per unit dark matter halo mass. Moreover, galaxies appear remarkably mature. In addition to their morphologies, scaling relations like the Baryonic Tully-Fisher and the dark matter fraction–surface brightness relation are already in place at early times. This clearly was not anticipated by models that expect disk galaxies to settle down only at later times. Not only were these scaling relations established early, they appear to have evolved little over most of cosmic time (the past ~ 11 Gyr back

to $z \approx 2.5$). This does not sit comfortably with the gradual assembly predicted by hierarchical galaxy formation (Fig. 1).

6.3. Structure Formation in MOND

The early formation of massive galaxies was explicitly predicted a quarter of a century ago by Sanders (1998). The new physics driving this prediction of accelerated structure formation is MOND, a theory that has had many other predictive successes (e.g., Sanders & Verheijen 1998; McGaugh & de Blok 1998; McGaugh 2011; McGaugh & Milgrom 2013a,b; Milgrom 2015; Sanders 2019a; McGaugh 2020; Mistele et al. 2024a,b). The nonlinearity of MOND causes growth to occur at a much higher rate early than expected with linear growth in Λ CDM (Sanders & McGaugh 2002).

MOND makes a number of long-standing predictions about early structure formation:

- an early cosmic dawn (McGaugh 2018, $z \approx 17$);
- massive galaxies at $z \gtrsim 10$ (Sanders 1998, 2008);
- early emergence of the cosmic web (by $z \approx 5$: Llinares et al. 2008);
- rich clusters of galaxies form by $z \approx 2$ (Sanders 1998);
- an enhanced ISW effect (McGaugh 2004);
- large voids swept clear by low redshift (McGaugh 2015);
- the largest scales forming at the present time (Sanders 1998) were anticipated to be comparable to Laniakea (Tully et al. 2014);
- the universe may depart from the isotropic ideal of the cosmological principle at late times (Felten 1984).

A number of puzzling observations in cosmology were anticipated by MOND, including the early formation of massive galaxies. The predictive power of MOND is not limited to the dynamics of individual galaxies.

Despite the predictive successes of MOND, we do not yet know how to construct a cosmology based on it. Perhaps the most promising theory to date is AeST, which has demonstrated the ability to fit the power spectrum (Skordis & Złośnik 2019) of both the cosmic microwave background and the large scale structure traced by galaxy redshift surveys. This is a significant accomplishment, since it had been thought that this was impossible without cold dark matter. Considerable work

remains to be done to see if AeST can be a fully satisfactory theory.

In contrast, Λ CDM provides a good fit to a wide range of cosmological observables, but does not provide a satisfactory explanation of the many phenomena that were predicted by MOND (Famaey & McGaugh 2012), nor is it clear that it can do so (Kroupa 2015; Sanders 2019b; McGaugh 2020; Merritt 2020, 2021; Roshan et al. 2021; Haslbauer et al. 2022a,b; Kroupa et al. 2024; Oehm & Kroupa 2024). We find ourselves caught between two very different theories that seem irreconcilable despite applying to closely related yet incommensurate lines of evidence (McGaugh 2015). The simple force law hy-

pothesized by MOND has made enough successful *a priori* predictions that it cannot be an accident, and must be telling us something. What that is remains as mysterious as the composition of dark matter.

This research has made use of data from a wide variety of sources, themselves enabled by great observatories like the Hubble Space Telescope, Spitzer, and JWST. We gratefully acknowledge the community and society that make these investigations possible. We also acknowledge conversations with many people, in particular Sara Tosi, Frances Duey, Konstantin Haubner, Tiffany Visgaitis, Tobias Mistele, Pengfei Li, and Marcel Pawlowski.

REFERENCES

- Adams, N. J., Conselice, C. J., Ferreira, L., et al. 2023, MNRAS, 518, 4755, doi: [10.1093/mnras/stac3347](https://doi.org/10.1093/mnras/stac3347)
- Anglés-Alcázar, D., Faucher-Giguère, C.-A., Kereš, D., et al. 2017, MNRAS, 470, 4698, doi: [10.1093/mnras/stx1517](https://doi.org/10.1093/mnras/stx1517)
- Angus, G. W., Famaey, B., & Buote, D. A. 2008, MNRAS, 387, 1470, doi: [10.1111/j.1365-2966.2008.13353.x](https://doi.org/10.1111/j.1365-2966.2008.13353.x)
- Angus, G. W., & McGaugh, S. S. 2008, MNRAS, 383, 417, doi: [10.1111/j.1365-2966.2007.12403.x](https://doi.org/10.1111/j.1365-2966.2007.12403.x)
- Arrabal Haro, P., Dickinson, M., Finkelstein, S. L., et al. 2023, Nature, 622, 707, doi: [10.1038/s41586-023-06521-7](https://doi.org/10.1038/s41586-023-06521-7)
- Asencio, E., Banik, I., & Kroupa, P. 2021, MNRAS, 500, 5249, doi: [10.1093/mnras/staa3441](https://doi.org/10.1093/mnras/staa3441)
- Atek, H., Shuntov, M., Furtak, L. J., et al. 2023, MNRAS, 519, 1201, doi: [10.1093/mnras/stac3144](https://doi.org/10.1093/mnras/stac3144)
- Balázs, L. G., Bagoly, Z., Hakkila, J. E., et al. 2015, MNRAS, 452, 2236, doi: [10.1093/mnras/stv1421](https://doi.org/10.1093/mnras/stv1421)
- Banik, I., & Zhao, H. 2022, Symmetry, 14, 1331, doi: [10.3390/sym14071331](https://doi.org/10.3390/sym14071331)
- Begeman, K. G., Broeils, A. H., & Sanders, R. H. 1991, MNRAS, 249, 523
- Behroozi, P., & Silk, J. 2018, MNRAS, 477, 5382, doi: [10.1093/mnras/sty945](https://doi.org/10.1093/mnras/sty945)
- Behroozi, P., Conroy, C., Wechsler, R. H., et al. 2020, MNRAS, 499, 5702, doi: [10.1093/mnras/staa3164](https://doi.org/10.1093/mnras/staa3164)
- Bell, E. F., Wolf, C., Meisenheimer, K., et al. 2004, ApJ, 608, 752, doi: [10.1086/420778](https://doi.org/10.1086/420778)
- Boylan-Kolchin, M. 2023, Nature Astronomy, 7, 731, doi: [10.1038/s41550-023-01937-7](https://doi.org/10.1038/s41550-023-01937-7)
- Boylan-Kolchin, M., Springel, V., White, S. D. M., Jenkins, A., & Lemson, G. 2009, MNRAS, 398, 1150, doi: [10.1111/j.1365-2966.2009.15191.x](https://doi.org/10.1111/j.1365-2966.2009.15191.x)
- Bregman, J. N., Temi, P., & Bregman, J. D. 2006, ApJ, 647, 265, doi: [10.1086/505190](https://doi.org/10.1086/505190)
- Carniani, S., Hainline, K., D'Eugenio, F., et al. 2024, arXiv e-prints, arXiv:2405.18485, doi: [10.48550/arXiv.2405.18485](https://doi.org/10.48550/arXiv.2405.18485)
- Casey, C. M., Akins, H. B., Shuntov, M., et al. 2023, arXiv e-prints, arXiv:2308.10932, doi: [10.48550/arXiv.2308.10932](https://doi.org/10.48550/arXiv.2308.10932)
- Castellano, M., Fontana, A., Treu, T., et al. 2022, ApJL, 938, L15, doi: [10.3847/2041-8213/ac94d0](https://doi.org/10.3847/2041-8213/ac94d0)
- . 2023, ApJL, 948, L14, doi: [10.3847/2041-8213/accea5](https://doi.org/10.3847/2041-8213/accea5)
- Cattaneo, A., Dekel, A., Faber, S. M., & Guiderdoni, B. 2008, MNRAS, 389, 567, doi: [10.1111/j.1365-2966.2008.13562.x](https://doi.org/10.1111/j.1365-2966.2008.13562.x)
- Clifton, T., Ferreira, P. G., Padilla, A., & Skordis, C. 2012, Physics Reports, 513, 1, doi: [10.1016/j.physrep.2012.01.001](https://doi.org/10.1016/j.physrep.2012.01.001)
- Clowes, R. G., Harris, K. A., Raghunathan, S., et al. 2013, MNRAS, 429, 2910, doi: [10.1093/mnras/sts497](https://doi.org/10.1093/mnras/sts497)
- Colin, J., Mohayaee, R., Rameez, M., & Sarkar, S. 2019, A&A, 631, L13, doi: [10.1051/0004-6361/201936373](https://doi.org/10.1051/0004-6361/201936373)
- Conselice, C. J., Mundy, C. J., Ferreira, L., & Duncan, K. 2022, ApJ, 940, 168, doi: [10.3847/1538-4357/ac9b1a](https://doi.org/10.3847/1538-4357/ac9b1a)
- de Blok, W. J. G., & McGaugh, S. S. 1997, MNRAS, 290, 533, doi: [10.1093/mnras/290.3.533](https://doi.org/10.1093/mnras/290.3.533)
- De Lucia, G., Springel, V., White, S. D. M., Croton, D., & Kauffmann, G. 2006, MNRAS, 366, 499, doi: [10.1111/j.1365-2966.2005.09879.x](https://doi.org/10.1111/j.1365-2966.2005.09879.x)
- Dekel, A., & Burkert, A. 2014, MNRAS, 438, 1870, doi: [10.1093/mnras/stt2331](https://doi.org/10.1093/mnras/stt2331)
- Di Teodoro, E. M., Fraternali, F., & Miller, S. H. 2016, A&A, 594, A77, doi: [10.1051/0004-6361/201628315](https://doi.org/10.1051/0004-6361/201628315)
- Di Teodoro, E. M., Posti, L., Ogle, P. M., Fall, S. M., & Jarrett, T. 2021, MNRAS, 507, 5820, doi: [10.1093/mnras/stab2549](https://doi.org/10.1093/mnras/stab2549)

- Di Teodoro, E. M., Posti, L., Fall, S. M., et al. 2023, MNRAS, 518, 6340, doi: [10.1093/mnras/stac3424](https://doi.org/10.1093/mnras/stac3424)
- Domènech, G., Mohayaee, R., Patil, S. P., & Sarkar, S. 2022, JCAP, 2022, 019, doi: [10.1088/1475-7516/2022/10/019](https://doi.org/10.1088/1475-7516/2022/10/019)
- Donnan, C. T., McLeod, D. J., Dunlop, J. S., et al. 2023, MNRAS, 518, 6011, doi: [10.1093/mnras/stac3472](https://doi.org/10.1093/mnras/stac3472)
- Donnan, C. T., McLure, R. J., Dunlop, J. S., et al. 2024, arXiv e-prints, arXiv:2403.03171, <https://arxiv.org/abs/2403.03171>
- Dressler, A., Oemler, Augustus, J., Couch, W. J., et al. 1997, ApJ, 490, 577, doi: [10.1086/304890](https://doi.org/10.1086/304890)
- Driver, S. P., Bellstedt, S., Robotham, A. S. G., et al. 2022, MNRAS, 513, 439, doi: [10.1093/mnras/stac472](https://doi.org/10.1093/mnras/stac472)
- Eggen, O. J., Lynden-Bell, D., & Sandage, A. R. 1962, ApJ, 136, 748, doi: [10.1086/147433](https://doi.org/10.1086/147433)
- Eilers, A.-C., Mackenzie, R., Pizzati, E., et al. 2024, arXiv e-prints, arXiv:2403.07986, doi: [10.48550/arXiv.2403.07986](https://doi.org/10.48550/arXiv.2403.07986)
- Famaey, B., & McGaugh, S. S. 2012, Living Reviews in Relativity, 15, 10, doi: [10.12942/lrr-2012-10](https://doi.org/10.12942/lrr-2012-10)
- Feix, M. 2016, PhRvD, 93, 104039, doi: [10.1103/PhysRevD.93.104039](https://doi.org/10.1103/PhysRevD.93.104039)
- Felten, J. E. 1984, ApJ, 286, 3, doi: [10.1086/162569](https://doi.org/10.1086/162569)
- Ferrara, A., Pallottini, A., & Dayal, P. 2023, MNRAS, 522, 3986, doi: [10.1093/mnras/stad1095](https://doi.org/10.1093/mnras/stad1095)
- Ferreira, L., Adams, N., Conselice, C. J., et al. 2022, ApJL, 938, L2, doi: [10.3847/2041-8213/ac947c](https://doi.org/10.3847/2041-8213/ac947c)
- Ferreira, L., Conselice, C. J., Sazonova, E., et al. 2023, ApJ, 955, 94, doi: [10.3847/1538-4357/acec76](https://doi.org/10.3847/1538-4357/acec76)
- Finkelstein, S. L. 2016, PASA, 33, e037, doi: [10.1017/pasa.2016.26](https://doi.org/10.1017/pasa.2016.26)
- Finkelstein, S. L., Bagley, M. B., Ferguson, H. C., et al. 2022a, arXiv e-prints, arXiv:2211.05792, doi: [10.48550/arXiv.2211.05792](https://doi.org/10.48550/arXiv.2211.05792)
- Finkelstein, S. L., Bagley, M. B., Haro, P. A., et al. 2022b, ApJL, 940, L55, doi: [10.3847/2041-8213/ac966e](https://doi.org/10.3847/2041-8213/ac966e)
- Finkelstein, S. L., Leung, G. C. K., Bagley, M. B., et al. 2023, arXiv e-prints, arXiv:2311.04279, doi: [10.48550/arXiv.2311.04279](https://doi.org/10.48550/arXiv.2311.04279)
- Franck, J. R. 2018, PhD thesis, Case Western Reserve University, Ohio
- Franck, J. R., & McGaugh, S. S. 2016a, ApJ, 817, 158, doi: [10.3847/0004-637X/817/2/158](https://doi.org/10.3847/0004-637X/817/2/158)
- . 2016b, ApJ, 833, 15, doi: [10.3847/0004-637X/833/1/15](https://doi.org/10.3847/0004-637X/833/1/15)
- . 2017, ApJ, 836, 136, doi: [10.3847/1538-4357/836/1/136](https://doi.org/10.3847/1538-4357/836/1/136)
- Franck, J. R., McGaugh, S. S., & Schombert, J. M. 2015, AJ, 150, 46, doi: [10.1088/0004-6256/150/2/46](https://doi.org/10.1088/0004-6256/150/2/46)
- Freeman, K. C. 1970, ApJ, 160, 811, doi: [10.1086/150474](https://doi.org/10.1086/150474)
- Glazebrook, K., Nanayakkara, T., Schreiber, C., et al. 2023, arXiv e-prints, arXiv:2308.05606, doi: [10.48550/arXiv.2308.05606](https://doi.org/10.48550/arXiv.2308.05606)
- Granett, B. R., Neyrinck, M. C., & Szapudi, I. 2008, ApJL, 683, L99, doi: [10.1086/591670](https://doi.org/10.1086/591670)
- Grazian, A., Fontana, A., Santini, P., et al. 2015, A&A, 575, A96, doi: [10.1051/0004-6361/201424750](https://doi.org/10.1051/0004-6361/201424750)
- Harikane, Y., Ouchi, M., Oguri, M., et al. 2023, ApJS, 265, 5, doi: [10.3847/1538-4365/acaaa9](https://doi.org/10.3847/1538-4365/acaaa9)
- Haslbauer, M., Banik, I., Kroupa, P., Wittenburg, N., & Javanmardi, B. 2022a, ApJ, 925, 183, doi: [10.3847/1538-4357/ac46ac](https://doi.org/10.3847/1538-4357/ac46ac)
- Haslbauer, M., Kroupa, P., Zonoozi, A. H., & Haghi, H. 2022b, ApJL, 939, L31, doi: [10.3847/2041-8213/ac9a50](https://doi.org/10.3847/2041-8213/ac9a50)
- Henriques, B. M. B., White, S. D. M., Thomas, P. A., et al. 2015, MNRAS, 451, 2663, doi: [10.1093/mnras/stv705](https://doi.org/10.1093/mnras/stv705)
- Horváth, I., Bagoly, Z., Hakkila, J., & Tóth, L. V. 2015, A&A, 584, A48, doi: [10.1051/0004-6361/201424829](https://doi.org/10.1051/0004-6361/201424829)
- Horváth, I., Hakkila, J., & Bagoly, Z. 2014, A&A, 561, L12, doi: [10.1051/0004-6361/201323020](https://doi.org/10.1051/0004-6361/201323020)
- Hubble, E. P. 1929, ApJ, 69, 103, doi: [10.1086/143167](https://doi.org/10.1086/143167)
- Katz, H., McGaugh, S., Teuben, P., & Angus, G. W. 2013, ApJ, 772, 10, doi: [10.1088/0004-637X/772/1/10](https://doi.org/10.1088/0004-637X/772/1/10)
- Katz, H., Rosdahl, J., Kimm, T., et al. 2023, The Open Journal of Astrophysics, 6, 44, doi: [10.21105/astro.2309.03269](https://doi.org/10.21105/astro.2309.03269)
- Kelleher, R., & Lelli, F. 2024, arXiv e-prints, arXiv:2405.08557, doi: [10.48550/arXiv.2405.08557](https://doi.org/10.48550/arXiv.2405.08557)
- Keller, B. W., Munshi, F., Trebitsch, M., & Tremmel, M. 2023, ApJL, 943, L28, doi: [10.3847/2041-8213/acb148](https://doi.org/10.3847/2041-8213/acb148)
- Kelson, D. D., Benson, A. J., & Abramson, L. E. 2016, arXiv e-prints, arXiv:1610.06566, <https://arxiv.org/abs/1610.06566>
- Knebe, A., & Gibson, B. K. 2004, MNRAS, 347, 1055, doi: [10.1111/j.1365-2966.2004.07182.x](https://doi.org/10.1111/j.1365-2966.2004.07182.x)
- Knebe, A., Pearce, F. R., Thomas, P. A., et al. 2015, MNRAS, 451, 4029, doi: [10.1093/mnras/stv1149](https://doi.org/10.1093/mnras/stv1149)
- Kovács, A., Beck, R., Szapudi, I., et al. 2020, MNRAS, 499, 320, doi: [10.1093/mnras/staa2631](https://doi.org/10.1093/mnras/staa2631)
- Kravtsov, A. V., & Borgani, S. 2012, ARA&A, 50, 353, doi: [10.1146/annurev-astro-081811-125502](https://doi.org/10.1146/annurev-astro-081811-125502)
- Kroupa, P. 2015, Canadian Journal of Physics, 93, 169, doi: [10.1139/cjp-2014-0179](https://doi.org/10.1139/cjp-2014-0179)
- Kroupa, P., Pflamm-Altenburg, J., Mazurenko, S., et al. 2024, arXiv e-prints, arXiv:2405.09609, doi: [10.48550/arXiv.2405.09609](https://doi.org/10.48550/arXiv.2405.09609)
- Krumholz, M. R., Burkhardt, B., Forbes, J. C., & Crocker, R. M. 2018, MNRAS, 477, 2716, doi: [10.1093/mnras/sty852](https://doi.org/10.1093/mnras/sty852)

- Kuhn, V., Guo, Y., Martin, A., et al. 2023, arXiv e-prints, arXiv:2312.12389, doi: [10.48550/arXiv.2312.12389](https://doi.org/10.48550/arXiv.2312.12389)
- Labbé, I., van Dokkum, P., Nelson, E., et al. 2023, *Nature*, 616, 266, doi: [10.1038/s41586-023-05786-2](https://doi.org/10.1038/s41586-023-05786-2)
- Lelli, F., De Breuck, C., Falkendal, T., et al. 2018, *MNRAS*, 479, 5440, doi: [10.1093/mnras/sty1795](https://doi.org/10.1093/mnras/sty1795)
- Lelli, F., Di Teodoro, E. M., Fraternali, F., et al. 2021, *Science*, 371, 713, doi: [10.1126/science.abc1893](https://doi.org/10.1126/science.abc1893)
- Lelli, F., McGaugh, S. S., & Schombert, J. M. 2016, *AJ*, 152, 157, doi: [10.3847/0004-6256/152/6/157](https://doi.org/10.3847/0004-6256/152/6/157)
- Lelli, F., McGaugh, S. S., Schombert, J. M., Desmond, H., & Katz, H. 2019, *MNRAS*, 484, 3267, doi: [10.1093/mnras/stz205](https://doi.org/10.1093/mnras/stz205)
- Lelli, F., Zhang, Z.-Y., Bisbas, T. G., et al. 2023, *A&A*, 672, A106, doi: [10.1051/0004-6361/202245105](https://doi.org/10.1051/0004-6361/202245105)
- Li, P., Tian, Y., Júlio, M. P., et al. 2023, *A&A*, 677, A24, doi: [10.1051/0004-6361/202346431](https://doi.org/10.1051/0004-6361/202346431)
- Llinares, C., Knebe, A., & Zhao, H. 2008, *MNRAS*, 391, 1778, doi: [10.1111/j.1365-2966.2008.13961.x](https://doi.org/10.1111/j.1365-2966.2008.13961.x)
- Lopez, A. M., Clowes, R. G., & Williger, G. M. 2022, *MNRAS*, 516, 1557, doi: [10.1093/mnras/stac2204](https://doi.org/10.1093/mnras/stac2204)
- Mancone, C. L., Gonzalez, A. H., Brodwin, M., et al. 2010, *ApJ*, 720, 284, doi: [10.1088/0004-637X/720/1/284](https://doi.org/10.1088/0004-637X/720/1/284)
- Marinacci, F., Vogelsberger, M., Pakmor, R., et al. 2018, *MNRAS*, 480, 5113, doi: [10.1093/mnras/sty2206](https://doi.org/10.1093/mnras/sty2206)
- McGaugh, S. S. 1999a, in *American Institute of Physics Conference Series*, Vol. 470, *After the Dark Ages: When Galaxies were Young (the Universe at $2 < z < 5$)*, ed. S. Holt & E. Smith, 72–76, doi: [10.1063/1.58637](https://doi.org/10.1063/1.58637)
- McGaugh, S. S. 1999b, *ApJ*, 523, L99, doi: [10.1086/312274](https://doi.org/10.1086/312274)
- . 2004, *ApJ*, 611, 26, doi: [10.1086/421895](https://doi.org/10.1086/421895)
- . 2011, *PRL*, 106, 121303, doi: [10.1103/PhysRevLett.106.121303](https://doi.org/10.1103/PhysRevLett.106.121303)
- . 2015, *Canadian Journal of Physics*, 93, 250, doi: [10.1139/cjp-2014-0203](https://doi.org/10.1139/cjp-2014-0203)
- . 2018, *PRL*, 121, 081305, doi: [10.1103/PhysRevLett.121.081305](https://doi.org/10.1103/PhysRevLett.121.081305)
- . 2020, *Galaxies*, 8, 35, doi: [10.3390/galaxies8020035](https://doi.org/10.3390/galaxies8020035)
- . 2022, *Triton Station*, 2201, 03, doi: [10.59350/emzn3-yzw39](https://doi.org/10.59350/emzn3-yzw39)
- . 2024, *Universe*, 10, 48, doi: [10.3390/universe10010048](https://doi.org/10.3390/universe10010048)
- McGaugh, S. S., & de Blok, W. J. G. 1998, *ApJ*, 499, 66
- McGaugh, S. S., Lelli, F., & Schombert, J. M. 2016, *PRL*, 117, 201101, doi: [10.1103/PhysRevLett.117.201101](https://doi.org/10.1103/PhysRevLett.117.201101)
- McGaugh, S. S., & Milgrom, M. 2013a, *ApJ*, 766, 22, doi: [10.1088/0004-637X/766/1/22](https://doi.org/10.1088/0004-637X/766/1/22)
- . 2013b, *ApJ*, 775, 139, doi: [10.1088/0004-637X/775/2/139](https://doi.org/10.1088/0004-637X/775/2/139)
- McGaugh, S. S., Schombert, J. M., Bothun, G. D., & de Blok, W. J. G. 2000, *ApJ*, 533, L99, doi: [10.1086/312628](https://doi.org/10.1086/312628)
- Melia, F. 2023, *MNRAS*, 521, L85, doi: [10.1093/mnras/slad025](https://doi.org/10.1093/mnras/slad025)
- Merlin, E., Fortuni, F., Torelli, M., et al. 2019, *MNRAS*, 490, 3309, doi: [10.1093/mnras/stz2615](https://doi.org/10.1093/mnras/stz2615)
- Merlin, E., Bonchi, A., Paris, D., et al. 2022, *ApJL*, 938, L14, doi: [10.3847/2041-8213/ac8f93](https://doi.org/10.3847/2041-8213/ac8f93)
- Merritt, D. 2020, *A Philosophical Approach to MOND: Assessing the Milgromian Research Program in Cosmology* (Cambridge University Press)
- . 2021, *Synthese*, 199, 8921, doi: [10.1007/s11229-021-03188-3](https://doi.org/10.1007/s11229-021-03188-3)
- Milgrom, M. 1983, *ApJ*, 270, 365, doi: [10.1086/161130](https://doi.org/10.1086/161130)
- . 2008, *NewAR*, 51, 906, doi: [10.1016/j.newar.2008.03.023](https://doi.org/10.1016/j.newar.2008.03.023)
- Milgrom, M. 2014, *Scholarpedia*, 9, 31410, doi: [10.4249/scholarpedia.31410](https://doi.org/10.4249/scholarpedia.31410)
- Milgrom, M. 2015, *PhRvD*, 92, 044014, doi: [10.1103/PhysRevD.92.044014](https://doi.org/10.1103/PhysRevD.92.044014)
- . 2018, *PhRvD*, 98, 104036, doi: [10.1103/PhysRevD.98.104036](https://doi.org/10.1103/PhysRevD.98.104036)
- . 2019, *PhRvD*, 99, 044041, doi: [10.1103/PhysRevD.99.044041](https://doi.org/10.1103/PhysRevD.99.044041)
- . 2021, *PhRvD*, 103, 044043, doi: [10.1103/PhysRevD.103.044043](https://doi.org/10.1103/PhysRevD.103.044043)
- Miller, S. H., Ellis, R. S., Sullivan, M., et al. 2012, *ApJ*, 753, 74, doi: [10.1088/0004-637X/753/1/74](https://doi.org/10.1088/0004-637X/753/1/74)
- Mistele, T., McGaugh, S., & Hossfelder, S. 2023, *A&A*, 676, A100, doi: [10.1051/0004-6361/202346025](https://doi.org/10.1051/0004-6361/202346025)
- Mistele, T., McGaugh, S., Lelli, F., Schombert, J., & Li, P. 2024a, *JCAP*, 2024, 020, doi: [10.1088/1475-7516/2024/04/020](https://doi.org/10.1088/1475-7516/2024/04/020)
- . 2024b, *ApJL*, 969, L3, doi: [10.3847/2041-8213/ad54b0](https://doi.org/10.3847/2041-8213/ad54b0)
- Mo, H. J., Mao, S., & White, S. D. M. 1998, *MNRAS*, 295, 319, doi: [10.1046/j.1365-8711.1998.01227.x](https://doi.org/10.1046/j.1365-8711.1998.01227.x)
- Mortonson, M. J., Hu, W., & Huterer, D. 2011, *PhRvD*, 83, 023015, doi: [10.1103/PhysRevD.83.023015](https://doi.org/10.1103/PhysRevD.83.023015)
- Naab, T., Johansson, P. H., & Ostriker, J. P. 2009, *ApJL*, 699, L178, doi: [10.1088/0004-637X/699/2/L178](https://doi.org/10.1088/0004-637X/699/2/L178)
- Nadathur, S., Hotchkiss, S., & Sarkar, S. 2012, *JCAP*, 2012, 042, doi: [10.1088/1475-7516/2012/06/042](https://doi.org/10.1088/1475-7516/2012/06/042)
- Naidu, R. P., Oesch, P. A., van Dokkum, P., et al. 2022, *ApJL*, 940, L14, doi: [10.3847/2041-8213/ac9b22](https://doi.org/10.3847/2041-8213/ac9b22)
- Naiman, J. P., Pillepich, A., Springel, V., et al. 2018, *MNRAS*, 477, 1206, doi: [10.1093/mnras/sty618](https://doi.org/10.1093/mnras/sty618)
- Nanayakkara, T., Glazebrook, K., Jacobs, C., et al. 2024, *Scientific Reports*, 14, 3724, doi: [10.1038/s41598-024-52585-4](https://doi.org/10.1038/s41598-024-52585-4)
- Neeleman, M., Prochaska, J. X., Kanekar, N., & Rafelski, M. 2020, *Nature*, 581, 269, doi: [10.1038/s41586-020-2276-y](https://doi.org/10.1038/s41586-020-2276-y)

- Nelson, D., Pillepich, A., Springel, V., et al. 2018, *MNRAS*, 475, 624, doi: [10.1093/mnras/stx3040](https://doi.org/10.1093/mnras/stx3040)
- . 2019, *MNRAS*, 490, 3234, doi: [10.1093/mnras/stz2306](https://doi.org/10.1093/mnras/stz2306)
- Nestor Shachar, A., Price, S. H., Förster Schreiber, N. M., et al. 2023, *ApJ*, 944, 78, doi: [10.3847/1538-4357/aca9cf](https://doi.org/10.3847/1538-4357/aca9cf)
- Newman, A. B., Ellis, R. S., Bundy, K., & Treu, T. 2012, *ApJ*, 746, 162, doi: [10.1088/0004-637X/746/2/162](https://doi.org/10.1088/0004-637X/746/2/162)
- Nipoti, C., Treu, T., Auger, M. W., & Bolton, A. S. 2009, *ApJL*, 706, L86, doi: [10.1088/0004-637X/706/1/L86](https://doi.org/10.1088/0004-637X/706/1/L86)
- Noordermeer, E., van der Hulst, J. M., Sancisi, R., Swaters, R. S., & van Albada, T. S. 2007, *MNRAS*, 376, 1513, doi: [10.1111/j.1365-2966.2007.11533.x](https://doi.org/10.1111/j.1365-2966.2007.11533.x)
- Nusser, A. 2002, *MNRAS*, 331, 909, doi: [10.1046/j.1365-8711.2002.05235.x](https://doi.org/10.1046/j.1365-8711.2002.05235.x)
- Nusser, A., Gubser, S. S., & Peebles, P. J. 2005, *PhRvD*, 71, 083505, doi: [10.1103/PhysRevD.71.083505](https://doi.org/10.1103/PhysRevD.71.083505)
- Oehm, W., & Kroupa, P. 2024, *Universe*, 10, 143, doi: [10.3390/universe10030143](https://doi.org/10.3390/universe10030143)
- Pallottini, A., & Ferrara, A. 2023, arXiv e-prints, arXiv:2307.03219, doi: [10.48550/arXiv.2307.03219](https://doi.org/10.48550/arXiv.2307.03219)
- Peebles, P. J. E. 1993, *Principles of Physical Cosmology* (Princeton University Press)
- Peebles, P. J. E., & Nusser, A. 2010, *Nature*, 465, 565, doi: [10.1038/nature09101](https://doi.org/10.1038/nature09101)
- Pelliccia, D., Tresse, L., Epinat, B., et al. 2017, *A&A*, 599, A25, doi: [10.1051/0004-6361/201629064](https://doi.org/10.1051/0004-6361/201629064)
- Peng, Y., Maiolino, R., & Cochrane, R. 2015, *Nature*, 521, 192, doi: [10.1038/nature14439](https://doi.org/10.1038/nature14439)
- Pillepich, A., Nelson, D., Hernquist, L., et al. 2018, *MNRAS*, 475, 648, doi: [10.1093/mnras/stx3112](https://doi.org/10.1093/mnras/stx3112)
- Pillepich, A., Nelson, D., Springel, V., et al. 2019, *MNRAS*, 490, 3196, doi: [10.1093/mnras/stz2338](https://doi.org/10.1093/mnras/stz2338)
- Pizzati, E., Hennawi, J. F., Schaye, J., & Schaller, M. 2024, *MNRAS*, 528, 4466, doi: [10.1093/mnras/stae329](https://doi.org/10.1093/mnras/stae329)
- Planck Collaboration, Aghanim, N., Akrami, Y., et al. 2020, *A&A*, 641, A6, doi: [10.1051/0004-6361/201833910](https://doi.org/10.1051/0004-6361/201833910)
- Rakos, K., Schombert, J., & Odell, A. 2008, *ApJ*, 677, 1019, doi: [10.1086/533513](https://doi.org/10.1086/533513)
- Renzini, A. 2006, *ARA&A*, 44, 141, doi: [10.1146/annurev.astro.44.051905.092450](https://doi.org/10.1146/annurev.astro.44.051905.092450)
- Rizzo, F., Vegetti, S., Fraternali, F., Stacey, H. R., & Powell, D. 2021, *MNRAS*, 507, 3952, doi: [10.1093/mnras/stab2295](https://doi.org/10.1093/mnras/stab2295)
- Rizzo, F., Vegetti, S., Powell, D., et al. 2020, *Nature*, 584, 201, doi: [10.1038/s41586-020-2572-6](https://doi.org/10.1038/s41586-020-2572-6)
- Rizzo, F., Roman-Oliveira, F., Fraternali, F., et al. 2023, *A&A*, 679, A129, doi: [10.1051/0004-6361/202346444](https://doi.org/10.1051/0004-6361/202346444)
- Robertson, B., Johnson, B. D., Tacchella, S., et al. 2023, arXiv e-prints, arXiv:2312.10033, doi: [10.48550/arXiv.2312.10033](https://doi.org/10.48550/arXiv.2312.10033)
- Rocca-Volmerange, B., Le Borgne, D., De Breuck, C., Fioc, M., & Moy, E. 2004, *A&A*, 415, 931, doi: [10.1051/0004-6361:20031717](https://doi.org/10.1051/0004-6361:20031717)
- Rodriguez-Gomez, V., Pillepich, A., Sales, L. V., et al. 2016, *MNRAS*, 458, 2371, doi: [10.1093/mnras/stw456](https://doi.org/10.1093/mnras/stw456)
- Roman-Oliveira, F., Fraternali, F., & Rizzo, F. 2023, *MNRAS*, 521, 1045, doi: [10.1093/mnras/stad530](https://doi.org/10.1093/mnras/stad530)
- Rosdahl, J., Katz, H., Blaizot, J., et al. 2018, *MNRAS*, 479, 994, doi: [10.1093/mnras/sty1655](https://doi.org/10.1093/mnras/sty1655)
- Rosdahl, J., Blaizot, J., Katz, H., et al. 2022, *MNRAS*, 515, 2386, doi: [10.1093/mnras/stac1942](https://doi.org/10.1093/mnras/stac1942)
- Roshan, M., Ghafourian, N., Kashfi, T., et al. 2021, *MNRAS*, 508, 926, doi: [10.1093/mnras/stab2553](https://doi.org/10.1093/mnras/stab2553)
- Rowland, L. E., Hodge, J., Bouwens, R., et al. 2024, arXiv e-prints, arXiv:2405.06025, doi: [10.48550/arXiv.2405.06025](https://doi.org/10.48550/arXiv.2405.06025)
- Sabti, N., Muñoz, J. B., & Kamionkowski, M. 2024, *PhRvL*, 132, 061002, doi: [10.1103/PhysRevLett.132.061002](https://doi.org/10.1103/PhysRevLett.132.061002)
- Sanders, R. H. 1998, *MNRAS*, 296, 1009, doi: [10.1046/j.1365-8711.1998.01459.x](https://doi.org/10.1046/j.1365-8711.1998.01459.x)
- . 2001, *ApJ*, 560, 1, doi: [10.1086/322487](https://doi.org/10.1086/322487)
- . 2003, *MNRAS*, 342, 901, doi: [10.1046/j.1365-8711.2003.06596.x](https://doi.org/10.1046/j.1365-8711.2003.06596.x)
- . 2007, *MNRAS*, 380, 331, doi: [10.1111/j.1365-2966.2007.12073.x](https://doi.org/10.1111/j.1365-2966.2007.12073.x)
- . 2008, *MNRAS*, 386, 1588, doi: [10.1111/j.1365-2966.2008.13140.x](https://doi.org/10.1111/j.1365-2966.2008.13140.x)
- . 2019a, *MNRAS*, 485, 513, doi: [10.1093/mnras/stz353](https://doi.org/10.1093/mnras/stz353)
- . 2019b, arXiv e-prints, arXiv:1912.00716, <https://arxiv.org/abs/1912.00716>
- Sanders, R. H., & McGaugh, S. S. 2002, *Ann. Rev. Astron. Astrophys.*, 40, 263, doi: [10.1146/annurev.astro.40.060401.093923](https://doi.org/10.1146/annurev.astro.40.060401.093923)
- Sanders, R. H., & Verheijen, M. A. W. 1998, *ApJ*, 503, 97, doi: [10.1086/305986](https://doi.org/10.1086/305986)
- Sankhyayan, S., Bagchi, J., Tempel, E., et al. 2023, *ApJ*, 958, 62, doi: [10.3847/1538-4357/acfaeb](https://doi.org/10.3847/1538-4357/acfaeb)
- Schechter, P. 1976, *ApJ*, 203, 297, doi: [10.1086/154079](https://doi.org/10.1086/154079)
- Schombert, J., McGaugh, S., & Lelli, F. 2019, *MNRAS*, 483, 1496, doi: [10.1093/mnras/sty3223](https://doi.org/10.1093/mnras/sty3223)
- Schombert, J., & Rakos, K. 2009, *ApJ*, 699, 1530, doi: [10.1088/0004-637X/699/2/1530](https://doi.org/10.1088/0004-637X/699/2/1530)
- Schombert, J. M. 2016, *AJ*, 152, 214, doi: [10.3847/0004-6256/152/6/214](https://doi.org/10.3847/0004-6256/152/6/214)
- Schramm, D. N. 1992, *Nuclear Physics B Proceedings Supplements*, 28, 243, doi: [10.1016/0920-5632\(92\)90180-Z](https://doi.org/10.1016/0920-5632(92)90180-Z)
- Schreiber, C., Glazebrook, K., Nanayakkara, T., et al. 2018, *A&A*, 618, A85, doi: [10.1051/0004-6361/201833070](https://doi.org/10.1051/0004-6361/201833070)
- Searle, L., & Zinn, R. 1978, *ApJ*, 225, 357, doi: [10.1086/156499](https://doi.org/10.1086/156499)

- Secrest, N. J., von Hausegger, S., Rameez, M., Mohayaee, R., & Sarkar, S. 2022, *ApJL*, 937, L31, doi: [10.3847/2041-8213/ac88c0](https://doi.org/10.3847/2041-8213/ac88c0)
- Secrest, N. J., von Hausegger, S., Rameez, M., et al. 2021, *ApJL*, 908, L51, doi: [10.3847/2041-8213/abdd40](https://doi.org/10.3847/2041-8213/abdd40)
- Shah, E. A., Lemaux, B., Forrest, B., et al. 2024, *MNRAS*, 529, 873, doi: [10.1093/mnras/stae519](https://doi.org/10.1093/mnras/stae519)
- Sharma, G., Freundlich, J., van de Ven, G., et al. 2023, arXiv e-prints, arXiv:2309.04541, doi: [10.48550/arXiv.2309.04541](https://doi.org/10.48550/arXiv.2309.04541)
- Shen, Y., Strauss, M. A., Oguri, M., et al. 2007, *AJ*, 133, 2222, doi: [10.1086/513517](https://doi.org/10.1086/513517)
- Skordis, C., & Złótnik, T. 2019, *PRD*, 100, 104013, doi: [10.1103/PhysRevD.100.104013](https://doi.org/10.1103/PhysRevD.100.104013)
- . 2021, *PhRvL*, 127, 161302, doi: [10.1103/PhysRevLett.127.161302](https://doi.org/10.1103/PhysRevLett.127.161302)
- Smit, R., Bouwens, R. J., Carniani, S., et al. 2018, *Nature*, 553, 178, doi: [10.1038/nature24631](https://doi.org/10.1038/nature24631)
- Somerville, R. S., & Kolatt, T. S. 1999, *MNRAS*, 305, 1, doi: [10.1046/j.1365-8711.1999.02154.x](https://doi.org/10.1046/j.1365-8711.1999.02154.x)
- Song, M., Finkelstein, S. L., Ashby, M. L. N., et al. 2016, *ApJ*, 825, 5, doi: [10.3847/0004-637X/825/1/5](https://doi.org/10.3847/0004-637X/825/1/5)
- Springel, V., White, S. D. M., Jenkins, A., et al. 2005, *Nature*, 435, 629, doi: [10.1038/nature03597](https://doi.org/10.1038/nature03597)
- Springel, V., Pakmor, R., Pillepich, A., et al. 2018, *MNRAS*, 475, 676, doi: [10.1093/mnras/stx3304](https://doi.org/10.1093/mnras/stx3304)
- Srisawat, C., Knebe, A., Pearce, F. R., et al. 2013, *MNRAS*, 436, 150, doi: [10.1093/mnras/stt1545](https://doi.org/10.1093/mnras/stt1545)
- Stachniewicz, S., & Kutschera, M. 2001, *Acta Physica Polonica B*, 32, 3629. <https://arxiv.org/abs/astro-ph/0110484>
- Starkman, N., Lelli, F., McGaugh, S., & Schombert, J. 2018, *MNRAS*, 480, 2292, doi: [10.1093/mnras/sty2011](https://doi.org/10.1093/mnras/sty2011)
- Stefanon, M., Bouwens, R. J., Labbé, I., et al. 2021, *ApJ*, 922, 29, doi: [10.3847/1538-4357/ac1bb6](https://doi.org/10.3847/1538-4357/ac1bb6)
- Steinhardt, C. L., Capak, P., Masters, D., & Speagle, J. S. 2016, *ApJ*, 824, 21, doi: [10.3847/0004-637X/824/1/21](https://doi.org/10.3847/0004-637X/824/1/21)
- Thomas, D., Maraston, C., Bender, R., & Mendes de Oliveira, C. 2005, *ApJ*, 621, 673, doi: [10.1086/426932](https://doi.org/10.1086/426932)
- Tian, Y., Ko, C.-M., Li, P., McGaugh, S., & Poblete, S. L. 2024, arXiv e-prints, arXiv:2402.12016, doi: [10.48550/arXiv.2402.12016](https://doi.org/10.48550/arXiv.2402.12016)
- Tripodi, R., Lelli, F., Feruglio, C., et al. 2023, *A&A*, 671, A44, doi: [10.1051/0004-6361/202245202](https://doi.org/10.1051/0004-6361/202245202)
- Tully, R. B., Courtois, H., Hoffman, Y., & Pomarède, D. 2014, *Nature*, 513, 71, doi: [10.1038/nature13674](https://doi.org/10.1038/nature13674)
- Tully, R. B., & Fisher, J. R. 1977, *A&A*, 54, 661
- Tully, R. B., Howlett, C., & Pomarède, D. 2023, *ApJ*, 954, 169, doi: [10.3847/1538-4357/aceaf3](https://doi.org/10.3847/1538-4357/aceaf3)
- van der Wel, A., Bell, E. F., van den Bosch, F. C., Gallazzi, A., & Rix, H.-W. 2009, *ApJ*, 698, 1232, doi: [10.1088/0004-637X/698/2/1232](https://doi.org/10.1088/0004-637X/698/2/1232)
- Wang, B., Fujimoto, S., Labbé, I., et al. 2023, *ApJL*, 957, L34, doi: [10.3847/2041-8213/acfe07](https://doi.org/10.3847/2041-8213/acfe07)
- Wang, B., Leja, J., de Graaff, A., et al. 2024, arXiv e-prints, arXiv:2405.01473, doi: [10.48550/arXiv.2405.01473](https://doi.org/10.48550/arXiv.2405.01473)
- Wardlow, J. 2021, *Science*, 371, 674, doi: [10.1126/science.abg2907](https://doi.org/10.1126/science.abg2907)
- Wechsler, R. H., & Tinker, J. L. 2018, *ARA&A*, 56, 435, doi: [10.1146/annurev-astro-081817-051756](https://doi.org/10.1146/annurev-astro-081817-051756)
- White, S. D. M., & Frenk, C. S. 1991, *ApJ*, 379, 52, doi: [10.1086/170483](https://doi.org/10.1086/170483)
- Wittenburg, N., Kroupa, P., Banik, I., Candlish, G., & Samaras, N. 2023, *MNRAS*, 523, 453, doi: [10.1093/mnras/stad1371](https://doi.org/10.1093/mnras/stad1371)
- Wittenburg, N., Kroupa, P., & Famaey, B. 2020, *ApJ*, 890, 173, doi: [10.3847/1538-4357/ab6d73](https://doi.org/10.3847/1538-4357/ab6d73)
- Wylezalek, D., Vernet, J., De Breuck, C., et al. 2014, *ApJ*, 786, 17, doi: [10.1088/0004-637X/786/1/17](https://doi.org/10.1088/0004-637X/786/1/17)
- Xu, Y., Ouchi, M., Yajima, H., et al. 2024, arXiv e-prints, arXiv:2404.16963, doi: [10.48550/arXiv.2404.16963](https://doi.org/10.48550/arXiv.2404.16963)
- Ying, J. M., Chaboyer, B., Boudreaux, E. M., et al. 2023, *AJ*, 166, 18, doi: [10.3847/1538-3881/acd9b1](https://doi.org/10.3847/1538-3881/acd9b1)
- Yung, L. Y. A., Somerville, R. S., Finkelstein, S. L., Popping, G., & Davé, R. 2019a, *MNRAS*, 483, 2983, doi: [10.1093/mnras/sty3241](https://doi.org/10.1093/mnras/sty3241)
- Yung, L. Y. A., Somerville, R. S., Finkelstein, S. L., Wilkins, S. M., & Gardner, J. P. 2023, *MNRAS*, doi: [10.1093/mnras/stad3484](https://doi.org/10.1093/mnras/stad3484)
- Yung, L. Y. A., Somerville, R. S., Popping, G., et al. 2019b, *MNRAS*, 490, 2855, doi: [10.1093/mnras/stz2755](https://doi.org/10.1093/mnras/stz2755)
- Yung, L. Y. A., Somerville, R. S., Ferguson, H. C., et al. 2022, *MNRAS*, 515, 5416, doi: [10.1093/mnras/stac2139](https://doi.org/10.1093/mnras/stac2139)
- Zolotov, A., Dekel, A., Mandelker, N., et al. 2015, *MNRAS*, 450, 2327, doi: [10.1093/mnras/stv740](https://doi.org/10.1093/mnras/stv740)